Available online at www.sciencedirect.com

ScienceDirect

Green Energy & Environment 1 (2016) 18–42

www.keaipublishing.com/gee

Review article

Progress in electrolytes for rechargeable Li-based batteries and beyond

Qi Li [a,1], Juner Chen [b,1], Lei Fan [b], Xueqian Kong [b], Yingying Lu [a,c,*]

[a] College of Chemical and Biological Engineering, Zhejiang University, Hangzhou 310027, China
[b] Department of Chemistry, Zhejiang University, Hangzhou 310027, China
[c] State Key Laboratory of Chemical Engineering, Zhejiang University, Hangzhou 310027, China

Received 9 February 2016; revised 13 March 2016; accepted 18 March 2016
Available online 13 April 2016

Abstract

Owing to almost unmatched volumetric energy density, Li-based batteries have dominated the portable electronic industry for the past 20 years. Not only will that continue, but they are also now powering plug-in hybrid electric vehicles and zero-emission vehicles. There is impressive progress in the exploration of electrode materials for lithium-based batteries because the electrodes (mainly the cathode) are the limiting factors in terms of overall capacity inside a battery. However, more and more interests have been focused on the electrolytes, which determines the current (power) density, the time stability, the reliability of a battery and the formation of solid electrolyte interface. This review will introduce five types of electrolytes for room temperature Li-based batteries including 1) non-aqueous electrolytes, 2) aqueous solutions, 3) ionic liquids, 4) polymer electrolytes, and 5) hybrid electrolytes. Besides, electrolytes beyond lithium-based systems such as sodium-, magnesium-, calcium-, zinc- and aluminum-based batteries will also be briefly discussed.
© 2016, Institute of Process Engineering, Chinese Academy of Sciences. Publishing services by Elsevier B.V. on behalf of KeAi Communications Co., Ltd. This is an open access article under the CC BY-NC-ND license (http://creativecommons.org/licenses/by-nc-nd/4.0/).

Keywords: Electrolyte; Ionic liquid; Polymer; Hybrid; Battery

1. Introduction

As a result of increased energy demand, such as increases in the price of refined fossil fuels and the environmental issues of their use, energy storage has become a growing global concern over the past decade. Electrochemical energy storage (EES) technologies based on batteries are beginning to show considerable promise as a result of many breakthroughs in the last few years due to their appealing features include high round-trip efficiency, flexible power, and energy characteristics to meet different grid functions, long cycle life, and low maintenance. Batteries such as rechargeable lithium batteries, redox-flow, and high temperature batteries, in particular, represent a viable energy storage technology for the integration of renewable resources that provide intermittent energy into the grid. Among them, Rechargeable lithium batteries especially Li-ion battery (LIB) have become successful and sophisticated energy storage devices since the first commercialization of lithium-ion batteries, carbon/lithium cobalt oxide ($LiCoO_2$) cell, in 1991 [1–4].

On the basis of the electrodes and electrolyte nature and physical state, several lithium-based battery classification schemes were proposed. Lithium battery (LB) is the common name given to primary (disposable) devices having lithium metal or a lithium compound as the anode. Lithium ion battery (LIB) indicates a family of secondary (rechargeable) devices where both the electrodes are intercalation materials, and the electrolyte is commonly a lithium salt dissolved in a mixture of organic solvents. Lithium air/O_2 battery (LAB) is a device where a lithium anode is electrochemically coupled with the atmosphere through a ceramic composite cathode, the electrolyte being liquid or polymer-based. The main advantage of this device is given by its very high specific energy,

* Corresponding author.
E-mail address: yingyinglu@zju.edu.cn (Y. Lu).
[1] Authors contribute equally.

http://dx.doi.org/10.1016/j.gee.2016.04.006
2468-0257/© 2016, Institute of Process Engineering, Chinese Academy of Sciences. Publishing services by Elsevier B.V. on behalf of KeAi Communications Co., Ltd. This is an open access article under the CC BY-NC-ND license (http://creativecommons.org/licenses/by-nc-nd/4.0/).

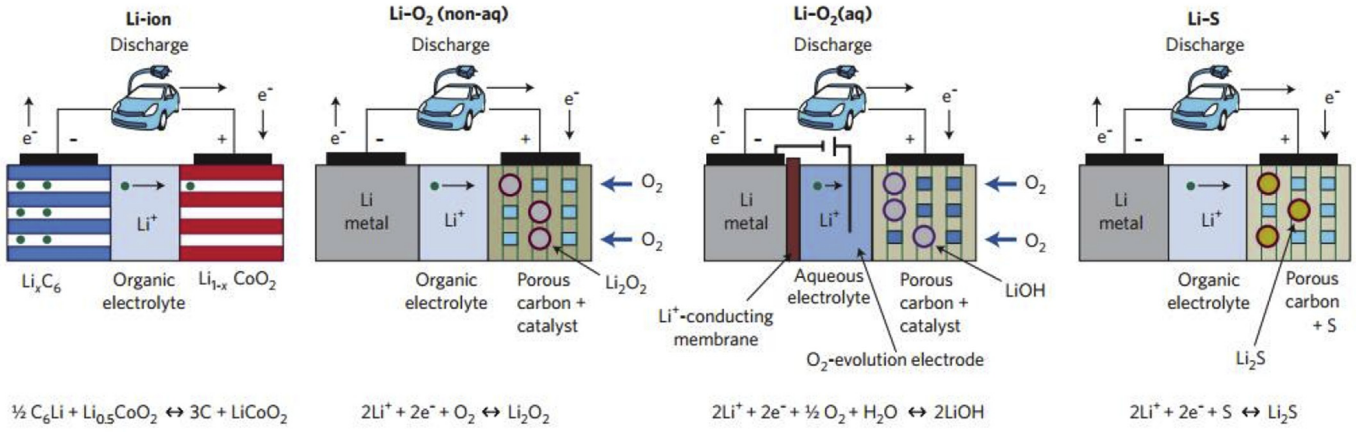

Fig. 1. Schematic representation of Li-ion, non-aqueous and aqueous Li−O_2 and Li−S batteries. Copyright 2012 Macmillan Publishers Limited.

11,140 Wh kg^{-1} (excluding oxygen), which is not far from that of the gasoline/air engine (11,860 Wh kg^{-1}). Another type of Li-based batteries of great interest is lithium sulfur batteries (LSB), which consist of a lithium metal anode, an organic liquid electrolyte, and a sulfur composite cathode. Sulfur, one of the most abundant elements on earth, is a promising cathode with the highest theoretical capacity of 1675 mAh g^{-1} among the solid elements. Moving from the traditional insertion cathodes to sulfur has many benefits besides the high capacity, such as the low operating voltage (2.15 V *vs.* Li^+/Li), low-cost, and environmentally friendly. An order of magnitude higher capacity than that of the conventional insertion compound cathodes can enable packaged LSB with an energy density of 400−600 Wh kg^{-1}, which is two or three times higher than that of current LIBs. Finally, other types of Li-based batteries such as lithium polymer battery (LPB) which is a rechargeable device where the lithium salt is somehow entrapped in a polymer (or composite) membrane, and lithium micro-battery (LM) which is an all solid state thin film device are also developed in recent years. Fig. 1 shows the Scheme of Li-ion, non-aqueous and aqueous Li−O_2 and Li−S batteries [4].

Inside a battery, the electrodes (mainly the cathode) are the limiting factors in terms of overall capacity, *i.e.* energy density, and cyclability. There has been impressive progress in the exploration of electrode materials for lithium-based batteries such as various metal oxides and polyanionic compounds as well as anode materials as shown in Fig. 2 [1,5,6]. The electrolyte, on the other hand, does determine the current (power) density, the time stability, and the safety of the battery since it is in close interaction with all the other components in the battery, including cathode, anode and separator. More importantly, the interface of the electrolyte with both the positive and the negative electrodes means its chemical stability requirements considerably limit the usable scope of material. Chemical compatibility is ensured through the formation of passivation layers, referred to as the solid electrolyte interface (SEI). The formation and physical properties of those

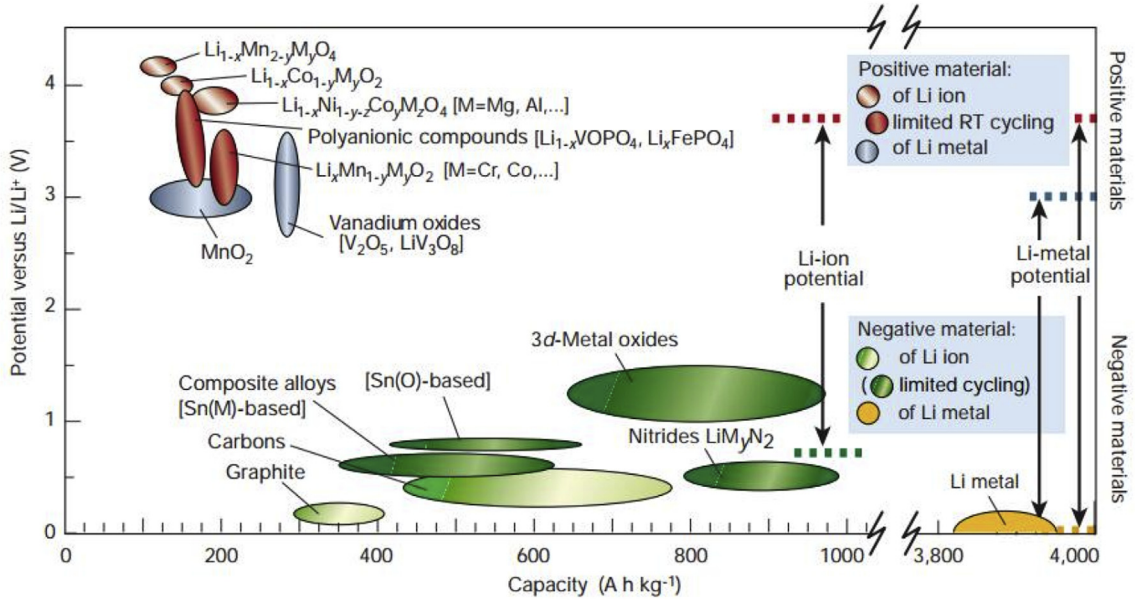

Fig. 2. Electrode materials presently used or under serious considerations for rechargeable lithium-based batteries. Copyright 2001 Macmillan Magazines Ltd.

protective layers depend on the nature of the electrode (especially the negative), thus implying that the study of electrolytes is not easily decoupled from the electrodes. Thus, more and more attentions have been paid to the investigation of the electrolyte which takes as the medium for transferring charges in battery.

An electrolyte could be viewed as the inert component in the battery, and it must demonstrate stability against both cathode and anode surface. During operation, the electrolyte should undergo no net chemical changes of the battery, and all Faradaic processes are expected to occur within the electrodes. Generally, an ideal electrolyte should meet the following minimal criteria: (1) It should be a good ionic conductor and electronic insulator, so that ion (Li^+) transport can be facile and self-discharge can be kept to a minimum; (2) It should have a wide electrochemical window, so that electrolyte degradation would not occur within the range of the working potentials of both the cathode and the anode; (3) It should also be inert to other cell components such as cell separators, electrode substrates, and cell packaging materials; (4) It should be thermally stable, for liquid electrolytes both the melting and boiling points should be well outside the operation temperatures; (5) It must have low toxicity and successfully meet also other measures of limited environmental hazard; (6) It must be based on sustainable chemistries, meaning that the elements are abundant and the synthesis processes are as low impact as possible, and (7) it must carry as low total cost, materials and production, as possible [7].

The electrolytes of interest for room temperature Li-based batteries can be classified into 1) non-aqueous electrolytes consisting of a lithium salt solubilized in an organic solvent or solvent mixture, 2) aqueous solution consisting of a lithium salt solubilized in water, 3) ionic liquids (ILs) consisting of an organic salt (R^+X^-) doped with a fraction of the lithium salt equivalent (Li^+X^-), 4) polymer electrolytes including gel polymer and solid polymer, and 5) hybrid electrolytes. In this review we will chiefly concentrate our attention on the development of electrolytes for Li-based batteries. Besides, electrolytes for beyond lithium such as sodium (Na)-, magnesium (Mg)-, calcium (Ca)-, zinc (Zn)- and aluminum (Al)-based batteries will also be briefly discussed.

2. Non-aqueous electrolytes

2.1. Non-aqueous electrolytes for Li-ion batteries

In the early 1990s, the rechargeable Li-ion battery was first introduced as a practicable product by the Sony Corporation commercially. Since that time, the technology of Li-ion battery has matured and dominated the consumer electronics market. Most of the electrolytes used in commercial lithium-ion batteries are non-aqueous solutions, in which Lithium hexafluorophosphate ($LiPF_6$) salt dissolved in organic carbonates, in particular, mixtures of ethylene carbonate (EC) with dimethyl carbonate (DMC), propylene carbonate (PC), diethyl carbonate (DEC), and/or ethyl methyl carbonate (EMC) [7]. In Table 1, the physicochemical properties of these common solvents are listed.

However, recent market demands for lithium-ion batteries with higher energy, power density, and safety which requires new organic solvents and lithium salts to enhance the property. The most efficient way is to increase the capacity and the voltage of the cells compared with other approaches. Searching for a high-voltage electrolyte has been much more important to develop lithium-ion batteries due to the low voltage stability of conventional carbonate solvents [8]. Lucht and co-workers [9] investigated the reaction of an electrolyte (1 M $LiPF_6$ in EC/DMC/DEC, 1:1:1) with the electrode of $LiNi_{0.5}Mn_{1.5}O_4$ (LNMO) at various voltages (4.0–5.3 V *vs.* Li) and found this common commercial electrolyte was unstable when charging above 4.5 V. In addition, the electrochemical performance of another conventional electrolyte of 1.2 M $LiPF_6$ dissolved in EC and EMC (3/7 in weight) under various charging conditions was reported [10]. It was found that this electrolyte easily decomposed above 4.9 V.

Organic fluoro-compounds are one of the most promising electrolyte solvents for high voltage condition, because fluorinated molecules have higher oxidation potentials due to the strong electron-withdrawing effect of the fluorine atom [8]. Zhang et al. [11] investigated the stability of different fluorinated electrolytes under high voltage conditions. It was found that the E5 electrolytes (1.2 M $LiPF_6$ in F-AEC/F-EMC/F-EPE (2/6/2)) have superior electrochemical stability compared with the EC/EMC-based Gen2 electrolyte. The test also showed the substitution of EMC with F-EMC and EC with F-AEC greatly improved the voltage limits of the electrolyte as shown in Fig. 3. The chemical structures of studied fluorinated carbonates and ethers are listed in Fig. 4.

The solid electrolyte interphase (SEI) is a protecting layer formed on the electrodes of a Li-ion battery mainly during the first few cycles. Once a SEI layer formed, it hinders further chemical reactions between electrodes and the electrolyte, thus reducing the consumption of active electrolyte and electrode materials. Battery performance, irreversible charge loss, rate capability, cycle ability, and safety could be significantly influenced by the quality of the SEI. A good SEI layer should

Table 1
The physicochemical properties of some common solvents.

Solvent	FW	d, g cm^{-3} (25 °C)	ε_r (25 °C)	η, mPa s (25 °C)	E_{homo}, eV	E_{lumo}, eV	mp, °C	bp, °C	fp, °C
Ethylene carbonate (EC)	88	1.32 (40 °C)	90 (40 °C)	1.9 (40 °C)	−12.86	1.51	36	238	143
Propylene carbonate (PC)	102	1.2	65	2.5	−12.72	1.52	−49	242	138
Dimethyl carbonate (DMC)	90	1.06	3.1	0.59	−12.85	1.88	5	90	17
Ethyl methyl carbonate (EMC)	104	1.01	3	0.65	−12.71	1.91	−53	108	23
Diethyl carbonate (DEC)	118	0.97	2.8	0.75	−12.59	1.93	−74	127	25

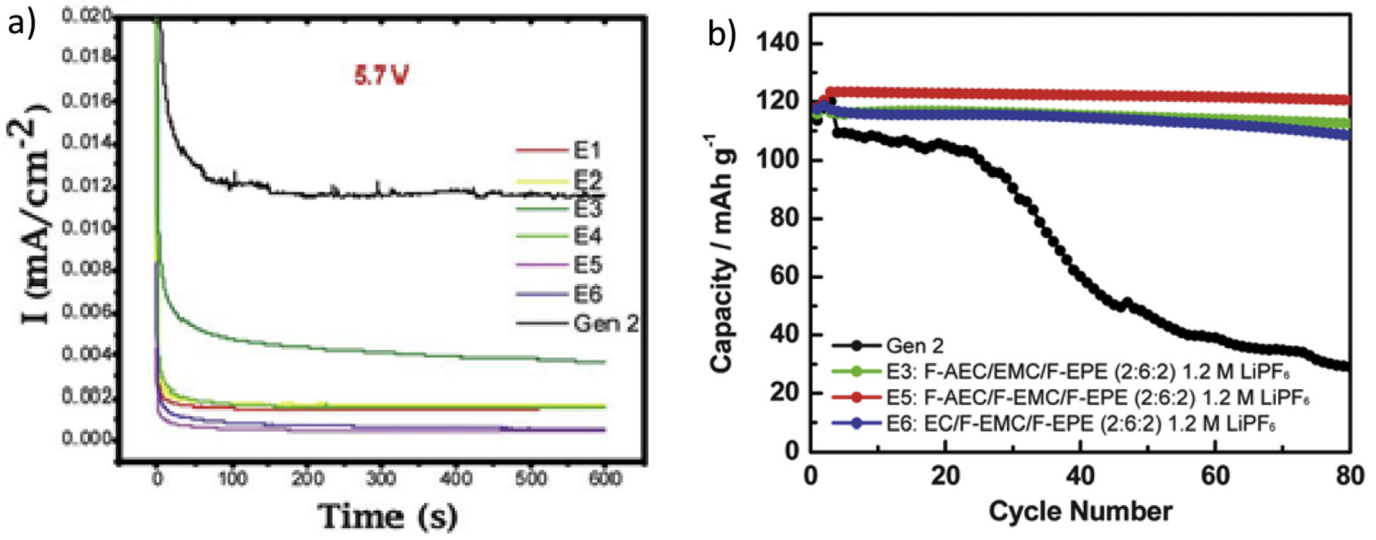

Fig. 3. (a) Electrochemical stability of Gen2 and fluorinated electrolytes E1–E6 at 5.7 V using a 3-electrode electrochemical cell. (b) Cycling capacity retention of $Li_4Ti_5O_{12}$ (LTO)/LNMO cells with baseline electrolyte Gen2 and fluorinated electrolytes E3, E5 and E6 at 55 °C. Gen2: 1.2 M $LiPF_6$ EC/EMC (3/7); E1: 1.2 M $LiPF_6$ in EC/EMC/F-EPE (2/6/2); E2: 1.2 M $LiPF_6$ in EC/EMC/F-EPE (2/5/3); E3: 1.2 M $LiPF_6$ in F-AEC/EMC/F-EPE (2/6/2); E4: 1.2 M $LiPF_6$ in F-AEC/EC/EMC/F-EPE (1/1/6/2); E5: 1.2 M $LiPF_6$ in F-AEC/F-EMC/F-EPE (2/6/2); E6: 1.2 M $LiPF_6$ in EC/F-EMC/F-EPE (2/6/2). Copyright 2013 The Royal Society of Chemistry.

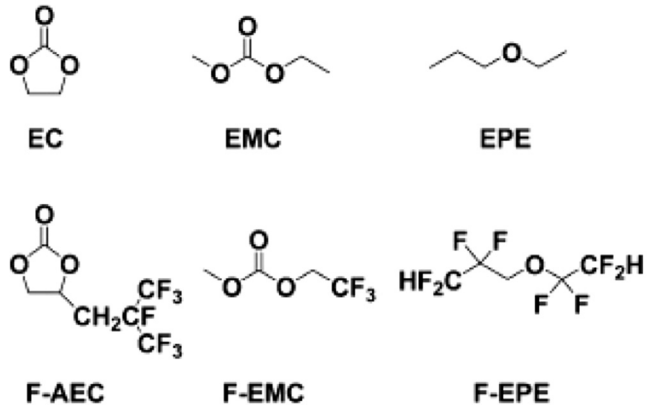

Fig. 4. Chemical structure of the baseline carbonate (EC and EMC), ethyl propyl ether (EPE), fluorinated cyclic carbonate (F-AEC), fluorinated linear carbonate (F-EMC), and fluorinated ether (F-EPE). Copyright 2013 The Royal Society of Chemistry.

be porous and ionic conductive, allowing favorable lithium ion transport. A typical SEI layer could include the combination of the following products: LiF, LiOH, Li_2CO_3, Li_2O and so forth [12]. On the basis of the idea of intentionally controlling thick solid electrolyte interface (SEI) and improving the property of Li-ion batteries, adding small amount of additives is also needed sometimes. Chen et al. [13] reported a novel non-aqueous $Li_2B_{12}F_{12-x}H_x$ electrolyte with the additive of lithium difluoro(oxalato)borate (LiDFOB), which had better property than the traditional electrolyte with $LiPF_6$ in cycle life and thermal stability. The $Li_2B_{12}F_9H_3$ electrolyte still had about 70% initial capacity at the condition of 55 °C with 1200 cycles. Another study reported by Xu and co-workers [14] gave a new way to improve the performance of EC/EMC, PC electrolyte which is mostly used by using tris (hexafluoro-iso-propyl) phosphate (HiFP) as additives, not only significantly improved the anodic stability of the electrolyte on a "5.0 V class" spinel $LiNi_{0.5}Mn_{1.5}O_4$ but also provided unexpected protective SEI chemistry on the graphitic anode.

In addition, a class of layer-structured transitional metal oxides $LiNi_{1-x-y}Co_xMn_yO_2$ has been investigated intensively and applied as key energy storage materials in Electric Vehicles (such as Tesla), due to their higher capacity, less toxicity and lower cost compared with $LiCoO_2$ [15]. A cell with a class of Li_2MnO_3-coated $LiNi_{0.5}Co_{0.2}Mn_{0.3}O_2$ cathode material and $LiPF_6$ (1 M) in a 1:1:1 (v/v/v) mixture of DMC, EMC and EC used as electrolyte was reported by Li and co-workers [16]. Suitable Li_2MnO_3-coated samples exhibit high Li^+ diffusion coefficient, excellent rate ability and enhanced cycling performance.

2.2. Non-aqueous electrolytes for Li–S batteries

Li–S batteries have been thought one of the most promising batteries for portable electronics due to their overwhelming advantage in energy density (2600 Wh kg^{-1} in theory). This value is up to five times as much as that of commercial LIBs. In addition, the resourceful and environmental-friendly elemental sulfur makes Li–S batteries more suitable in modern society in consideration of cost and protecting the environment [4,17].

However, Li–S cells using organic electrolytes usually show poor cycle performances and low Columbic efficiencies because of the formation of various lithium polysulfide species (Li_2S_n, $n = 2–8$) which are soluble in organic electrolytes. Searching the more suitable non-aqueous electrolytes for Li–S batteries is necessary [18].

Organic electrolytes containing lithium salts (e.g., lithium perchlorate ($LiClO_4$), $LiPF_6$, lithium trifluoromethanesulfonate ($LiCF_3SO_3$), or lithium bistrifluoromethylsulfonyl imide ($Li(CF_3SO_2)_2N$)) and a mixture of cyclic or linear ethers as solvents (e.g., tetrahydrofuran (THF), 1,3-dioxolane (DOL), dimethoxy ethane (DME), and tetra(ethylene glycol)dimethyl ether (TEGDME)) are commonly used for Li–S batteries [19].

Gao et al. [20] found the solvents in the electrolyte for Li–S battery played an important role in affecting the electrochemical performance but the lithium salts had no obvious effects. Such ethereal solvents (DOL/DME and TEGDME) with low-viscosity could be appropriate solvents because they can lead to the reduction of soluble polysulfides completely during cycles. Moreover, X-ray absorption spectra (XAS) revealed that reduced sulfur species could chemically react with carbonate based solvents such as EC, PC and DEC, making them unsuitable for Li–S batteries. The cycling performance of different solvents is shown in Fig. 5.

When the ethereal electrolytes are with high solubility of polysulfide, the Li–S battery can operate with a high concentration of polysulfides and the soluble polysulfides can react with Li and possibly suppress the growth of Li dendrite as well. However this may also cause both Li corrosion and the internal polysulfide shuttle because of their relatively high solubility [21]. Recently, much attention has been given to Li salts such as lithium bis(trifluoromethanesulfonyl)imide (LiTFSI) because their good thermal stability and excellent hydrolytic stability comparing with the $LiPF_6$ which is popularly used [22]. Hu et al. [23] reported a new "solvent-in-salt" electrolyte with 7 M LiTFSI in DOL/DME per solvent which is a super high salt concentration. The Li–S battery with this electrolyte showed a 1041 mAh g^{-1} initial specific discharge capacity while the Coulombic efficiency was 93.7% in the first cycle. The improvement may because the nearly saturated LiTFSI can hardly dissolve the intermediate products and thus avoid Li polysulfides shuttle.

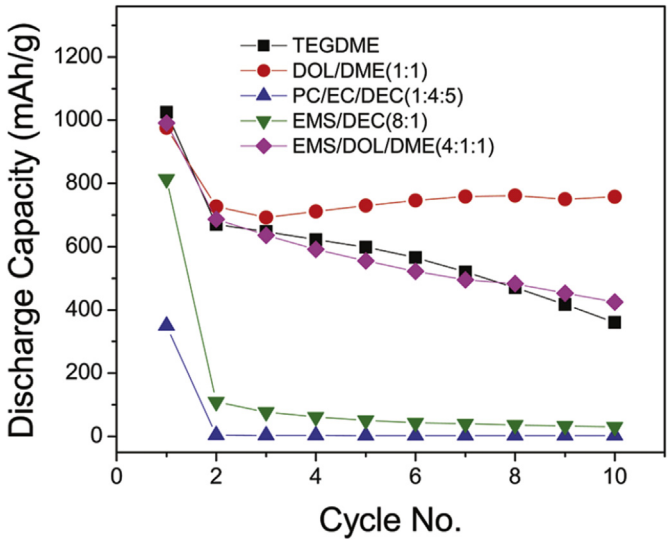

Fig. 5. Cycling performance of sulfur/carbon composites in 1.0 M $LiCF_3SO_3$ with different solvents. Copyright 2011 American Chemical Society.

Recent researches have also studied the relationship between the volume of electrolytes and the cycling performance of Li–S batteries. Cheng et al. [24] reported a lithium-sulfur cell with a high initial discharge capacity of 1053 mAh g^{-1} and an ultralow decay rate of 0.049%/per cycle during 1000 cycles was obtained by matching the sulfur/electrolyte loading. Brückner et al. [25] demonstrated how an excess amount of electrolyte in combination with a high rate and low sulfur loading can lead to an increase in cycle life and capacity retention as well. That is an easy way to tune the shuttle of polysulfide, which provides new insights to improvement of the lithium sulfur battery technology.

Compared to the roles played by additives in Li-ion batteries, the additives used in Li–S cells are fewer in numbers, but still urgently needed. Additives can have significant effect on Li–S performance by reducing the shuttle mechanism arising from the dissolution of polysulfides in the liquid electrolyte. The most prominent example is lithium nitrate ($LiNO_3$), which has been introduced to stabilize the Li anode by a protective layer formed on the anode surface [26]. The $LiNO_3$ can reduce into insoluble Li_xNO_y species, oxidize the sulfides to Li_xSO_y species, and passivate the Li electrode which prevent the continuous reaction between the polysulfides and Li [27]. Phosphorus pentasulfide (P_2S_5) can also be used as the additive of electrolytes. It can help to develop a dense and smooth passivation layer on the surface of the Li anode with high Li^+ conductivity and to prevent the insoluble Li_2S and Li_2S_2 from precipitating. In addition, P_2S_5 can react with Li_2S_n ($n = 1–8$) which turns to soluble complexes and converts the insoluble Li_2S and Li_2S_2 into highly soluble complexes by this way [28]. Recent report shows that the hybrid additives of $LiNO_3$ and Li polysulfide can lead to the improvement in cycling performance. The synergetic effect of both $LiNO_3$ and lithium polysulfide is beneficial to form dense and stable SEI layer which prevented dendrite growth and reduced electrolyte decomposition [29,30].

3. Aqueous electrolytes

3.1. Aqueous electrolytes for Li-ion batteries

The LIBs with organic electrolytes have been applied in portable electronic devices, electronic devices and power storage owing to its wide electrochemical stability, high voltages, and excellent energy density. However, organic electrolytes are flammable which limits its application for LIBs on larger scales. Using aqueous electrolytes with higher ionic conductivity instead of the flammable organic electrolytes is thought the most promising approach because of the internally environmental, non-flammable and low cost property [31–33].

In the mid-1990s, the lithium nitrate ($LiNO_3$) aqueous electrolyte was first to be used by the Dahn group [34–36] to construct an aqueous rechargeable lithium-ion battery (ARLB). Unfortunately, this system shows poor cycling performance. The narrow electrochemical stability window (1.23 V) of liquid water limits the success of aqueous

electrolyte for lithium batteries. Since then, several ARLB systems using different aqueous electrolytes such as $LiNO_3$ and lithium sulfate (Li_2SO_4) with suitable electrodes to acquire better cycle ability and higher rate capability are reported. Zhao et al. [37] further investigated the system of 9 M $LiNO_3$ aqueous solution with the cathode $LiFePO_4$/C and anode LiV_3O_8. It delivered a capacity of 88.7 mAh g^{-1} at the rate of 10 C after 100 cycles and a discharge capacity of 60 mAh g^{-1} at the rate of 50 C after 500 cycles. Another kind of aqueous electrolytes, Li_2SO_4 was also reported [38]. It exhibited over 90% capacity retention up to 1000 cycles consisting of $LiTi_2(PO_4)_3$–$LiFePO_4$ in 0.5 M Li_2SO_4 aqueous solution by eliminating oxygen in order to adjust the pH values of the electrolyte. In addition, Wang et al. [39] reported that a way which used the coating consisted of a LISICON and gel polymer electrolyte (GPE) film to protect Li metal from the Li_2SO_4 aqueous solution. Because of the "cross-over" effect of Li^+ ions in the coating, the lithium battery delivered a high output voltage (4.0 V) and high energy density (446 Wh k^{-1}). The value was much higher than that of conventional Li-ion batteries.

Recently, a new "water-in-salt" aqueous electrolyte was report [40]. It was obtained by dissolving LiTFSI at extremely high concentrations (molality >20 m) in water whose electrochemical window was extended to ~3.0 V due to the formation of an interphase between the electrode and electrolyte. The interphases were formed by manipulating the source of electrolyte decomposition during the initial charging processes. Illustration of expanded electrochemical stability window for water-in-salt electrolytes is shown in Fig. 6(B). A full lithium-ion battery of 2.3 V using such an aqueous electrolyte which was demonstrated to have almost 100% coulombic efficiency with more than 1000 cycles could compete with the conventional non-aqueous Li-ion batteries in terms of power and energy density. Fig. 6(A) shows the performance of aqueous Li-ion batteries based on various electrochemical couples.

3.2. Aqueous electrolytes for Li–air batteries

Lithium–air secondary batteries are attracting growing attention because of their extremely high energy density about 11,680 Wh kg^{-1} in theory. Nonetheless, Li-air batteries using non-aqueous electrolytes always show poor cycle life and low practical energy density. The reason is that the insoluble discharge products easily clog the porous air cathode and the electrolytes decompose during cycling [41,42]. Therefore, many researchers have been focused on using aqueous electrolyte for lithium–air batteries.

If lithium metal is in contact with electrolyte at a potential lower than −3.040 V *vs.* Normal Hydrogen Electrode (NHE), then water will not be decomposed [43]. According to this, Visco et al. [44] reported a concept of the water stable lithium electrode. This concept introduced a NASICON-type lithium ion conducting solid electrolyte, $Li_{1+x}A_xM_{2-x}(PO_4)_3$ (A = Al, Sc, Y, M = Ti, Ge), as a protective layer that covered and prevented the lithium metal from direct contact with the aqueous electrolytes. $Li_{1+x}Al_xTi_{2-x}$ $(PO_4)_3$ (LTAP) and $Li_{1.4}Al_{0.4}Ge_{1.6}$ $(PO_4)_3$ (LAGP) were unstable in an aqueous solution of 1 M LiOH, but stable in that saturated with lithium hydroxide (LiOH) and lithium chloride (LiCl) [45,46]. Hirokazu et al. [47] proposed a study about the different performance of the aqueous solution of saturated LiOH with 10 M LiCl against various carbon materials. Carbon with a high surface, such as Ketjen black, delivered stable electrode potentials for the oxygen reduction reaction (ORR) during a long polarization process.

In order to make full use of the aqueous electrolytes and minimizing the risk of lithium in contact with water at the same time, a mixed electrolyte design was suggested by Zhou and co-workers [48] recently. The cathode was in contact with the aqueous electrolytes while the lithium anode in contact with the organic electrolyte. A Li^+ conducting glass ceramic membrane (LISICON) was between the two kinds of electrolytes. The lithium anode was protected by LISICON, which

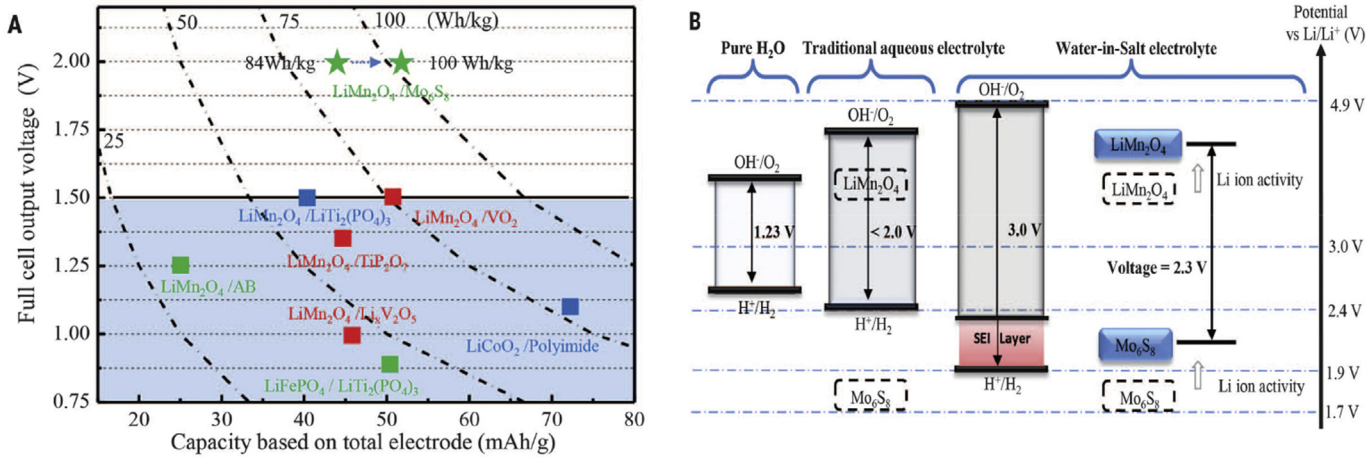

Fig. 6. (A) Performance of aqueous Li-ion batteries based on various electrochemical couples. Color code for cycling stability: red, <100 cycles; blue, 100–200 cycles; green, >1000 cycles. (B) Illustration of expanded electrochemical stability window for water-in-salt electrolytes together with the modulated redox couples of $LiMn_2O_4$ cathode and Mo_6S_8 anode caused by high salt concentration. Copyright 2015 American Association for the Advancement of Science.

prevented the violent reaction between lithium and water. This design exhibited a very long discharge time about 500 h with a capacity of 50,000 mA h g^{-1}.

4. Ionic liquid electrolytes

4.1. ILs as electrolytes for Li-ion batteries

Room-temperature ionic liquids (ILs) recently have attracted much more attention as electrolytes for next-generation LIBs, mainly because of their non-volatile and non-flammable nature. They promise one kind of safer electrolytes compared with conventional organic liquid based electrolytes in terms of thermal properties. ILs also exhibit many interesting properties, including high ion conductivity, great chemical and electrochemical stability, large electrochemical stability window (ESW), and large solubility of organic and inorganic compounds [49,50]. The drawbacks with ILs in electrolytes are their much higher viscosities than organic liquids which result in reduced conductivities/mobility and they are at a relatively larger cost than any organic solvents. Recent literatures proposed some possible ways to solve these problems such as searching for new cations and anions, mixtures with traditional organic carbonates.

ILs have a mass of combinations of cations and anions. Common cations used for ionic liquid electrolytes are imidazolium, quaternary ammonium, pyrrolidinium and piperidinium, while anions are PF_6^-, BF_4^-, bis(trifluoromethanesulfonyl)imide ($TFSI^-$) and so on. These kinds of ILs electrolytes for LIBs are extensively studied experimentally and theoretically.

4.1.1. Imidazolium based ILs

Imidazolium based ILs has the advantages of low viscosity and relatively high electrical conductivity which at 25 °C is usually greater than 10^{-3} S cm^{-1}. Nevertheless, Imidazolium based cations always suffer from cathodic instabilities. Imidazolium based ILs also have relatively narrow stability window of about 4 V (*vs.* Li/Li^+) and have poor electrochemical stability. In addition, this system usually has high reduction potential at about 1 V (*vs.* Li/Li^+) which is higher than the deposition potential of Li, so metallic lithium cannot directly works as the cathode of the battery in the system. There have been a lot of researches concerning ionic liquids involving imidazolium cation as solvent of lithium salts in electrolytes. Some of them pointed out that the electrochemical stability is limited by reduction potential, especially due to the presence of an acidic C2 proton of imidazolium cation [51]. Sun et al. [52] reported a study about 1-ethyl-2,3-trimethyleneimidazolium bis(trifluoromethane sulfonyl)imide ([ETMIm][TFSI]), and reference imidazolium compounds, 1-ethyl-3-methylimidazolium bis(trifluoromethanesulfonyl) imide ([EMIm][TFSI]) and 1, 2-dimethyl-3-butylimidazolium bis(trifluoromethanesulfonyl)imide ([DMBIm][TFSI]) as solvents for Li-ion batteries so as to investigate the relationship between electrochemical properties and the alkylation at the C-2 position of the imidazolium ring. Final results showed that

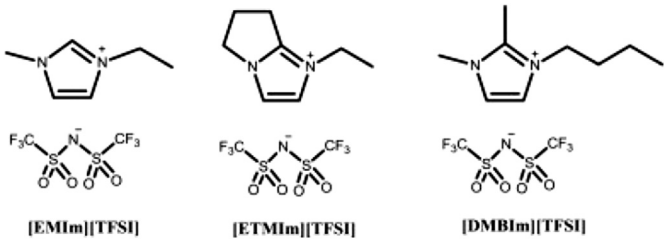

Fig. 7. Structures of these three imidazolium based ionic liquids. Copyright 2013 Elsevier.

[ETMIm][TFSI] has better reductive stability than the other two ILs because its unique structure as shown in Fig. 7.

The effect of various substituents on imidazolium based ILs have resulted in improved physical properties, for instance cycloalkyl substituted imidazolium ILs are superior to n-alkyl substituted ILs [53] and alkoxy functionalized imidazolium-based ILs have shown promising characteristics than their alkyl counterparts [54].

Some imidazolium based ILs, such as 1-allyl-3-vinyl imidazolium bis(trifluoromethanesulphonyl)imide ([AVIm][TFSI]) [55], have been used as solvents or additives in organic carbonate electrolyte and the results show a stable and dense polymer film which can prevent electrolyte and cathode from oxidative decomposition. In the term of anions, the bis(trifluoromethylsulfonyl)imide (NTf_2^-) turn to be used instead of bis(trifluoromethanesulfonyl)imide ($TFSI^-$) even if some drawbacks exist about its corrosive characters. However, it has advantages such as high thermal stability and low viscosity particularly [56].

4.1.2. Quaternary ammonium based ILs

Compared with imidazolium based ILs, quaternary ammonium based ILs has better electrochemical stability (low cathodic limiting potential), and its electrochemical stability window is usually greater than 5 V (*vs.* Li/Li^+). Therefore, this kind of ILs may withstand the lithium electrochemical deposition and dissolution without reduction reaction of decomposition on itself and can be as electrolyte for high voltage of Li-ion batteries. However, quaternary ammonium based ILs may be limited in application because of the larger size of cations, high viscosity and low ionic conductivity.

Introducing functional groups into cations can signally altering the physicochemical properties of ionic liquids. Compared with other functional groups, such as nitrile- and ester-functionalized ILs, ether group [57] can not only facilitate to reduce the viscosities and melting points of ionic liquids but also not lead to the decline of electrochemical stability of ionic liquids obviously. The number of ether group usually is one or two, because too much ether base with big size of quaternary ammonium cation will resulted in increasing the polarity of the cation and improving Van der Waals interactions between anions and cation, which cause high viscosity and going against the performance of lithium battery instead [58]. For quaternary ammonium ILs, the most well-known IL is *N*, *N*-diethyl-*N*-methyl-*N*-(2-methoxyethyl) ammonium TFSA (DEME–TFSA) [59].

Another good way to design safer electrolytes based on ILs which show better properties including low viscosity, thermal stability and electrochemical stability, is to introduce organic solvents as additives [60]. Reports showed that 20 wt% EC could not accelerate the accelerated degradation of quaternary ammonium based IL, but could decrease the viscosity as well as improves the electrochemical window stability.

4.1.3. Pyrrolidinium and piperidinium based ILs

Pyrrolidinium and piperidinium based ILs have similar physicochemical properties with ammonium based ILs, such as good electrochemical stability, relatively low viscosity and higher ionic conductivity [61]. In addition, the five-membered rings of pyrrolidinium has smaller size than the six-membered rings of piperidinium when the branched chain of cation and the structure of anion are the same, therefore pyrrolidinium base ILs tend to have lower viscosity.

Fang et al. [62] synthesized and characterized four kinds of ILs based on pyrrolidinium and piperidinium cations and $TFSI^-$ anion as shown in Fig. 8. Results drew the same conclusion because the viscosities of P(2o1)2−TFSI (55 mPa s) and P(2o1)(2o2)−TFSI (53 mPa s) were lower than that of PP(2o1)2−TFSI (122 mPa s) and PP(2o1)(2o2)−TFSI (111 mPa s) at 25 °C. Using these IL electrolytes in Li/$LiFePO_4$ cells delivered good cycle performance and discharge capacity.

N-Methyl-*N*-butylpyrrolidinium bis(trifluoromethylsufonyl) imide ([PYR_{14}][TFSI]) is one of the pyrrolidinium based ILs which has been extensively studied recently [63]. Its viscosity is 60 mPa s, electrical conductivity is 2.59 mS cm^{-1} and electrochemical stability window is 5.76 V (*vs.* Li/Li^+) at 30 °C. In addition, the high decomposition temperature (>400 °C) and non-flammability make it a promising electrolyte for using in high-safety Li batteries. It is also indicated in literature that the Li salt concentration in the IL greatly affects the capacity, rate capability, and cycle life of the electrode [64]. In order to alleviate its high viscosity and low conductivity at room temperature, three types of organic additives, namely vinylene carbonate (VC), gamma-butyrolactone (γ-BL), and propylene carbonate (PC) were introduced [64] into the PYR_{14}−TFSI-based IL electrolyte. γ-BL was found to be more effective than VC and PC in the IL electrolyte to improve cell capacity, rate capability, and cycling performance.

Compared with PYR_{14}−TFSI, *N*-methyl-*N*-propylpiperidinium bis(trifluoromethanesulfonyl) imide (PP_{13}−TFSI), one of the piperidinium based ILs, has lower decomposition voltage of reduction (0.3 V *vs.* Li/Li^+) and is relatively stable for metallic lithium anode. The electrochemical performance of this kind of electrolyte with high capacity cathode Li$[Li_{0.2}Mn_{0.54}Ni_{0.13}Co_{0.13}]O_2$ have been investigated by Li et al. [65] With the concentration of PP_{13}TFSI increased, the irreversible capacity loss decreased and the coulomb efficiency increased. This results showed that PP_{13}TFSI-added electrolyte can be used for Li-rich cathode material and reduce the safety concern of lithium-ion battery.

4.1.4. Other kinds of ILs

In addition to the ILs above, there are some other kinds of ILs as solvent electrolytes used in lithium ion battery such as pyrazolium based ILs [66]. The C−N heterocyclic structure of pyrazolium cation is similar to that of imidazolium cation except the different positions of the two N atoms. However, studies involving pyrazolium ILs are quite rare by contrast with imidazolium ILs. Chai et al. [67] synthesized four kinds of ILs based on pyrazolium cations and $TFSI^-$ anions as shown in Fig. 9. These four ILs have low melting point and low viscosity. Moreover, literature results also showed these IL electrolytes are stable for lithium metal with 0.4 mol kg^{-1} LiTFSI.

Two kinds of ILs based on guanidinium (1g (2o1) (2o1)−TFSA, 1g (2o1) (2o2)−TFSA, either TFSA or TFSI is short for bis(trifluoromethanesulfonyl)imide) were investigated by Jin et al. [58]. Fig. 10 shows the structures of cations and anion of the two guanidinium based ILs. The two IL electrolytes all delivered good cycle performance at 25 °C and 55 °C.

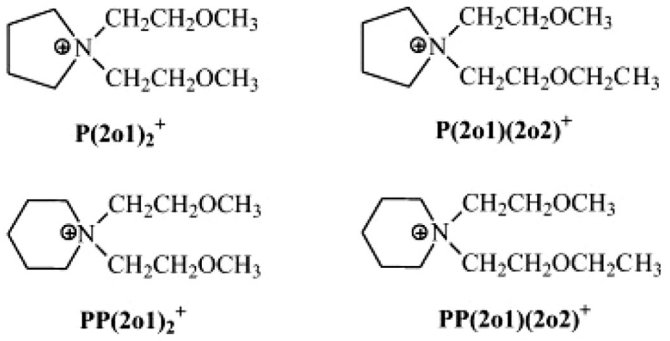

Fig. 8. Structures of cations of the four functionalized ILs. Copyright 2011 Elsevier.

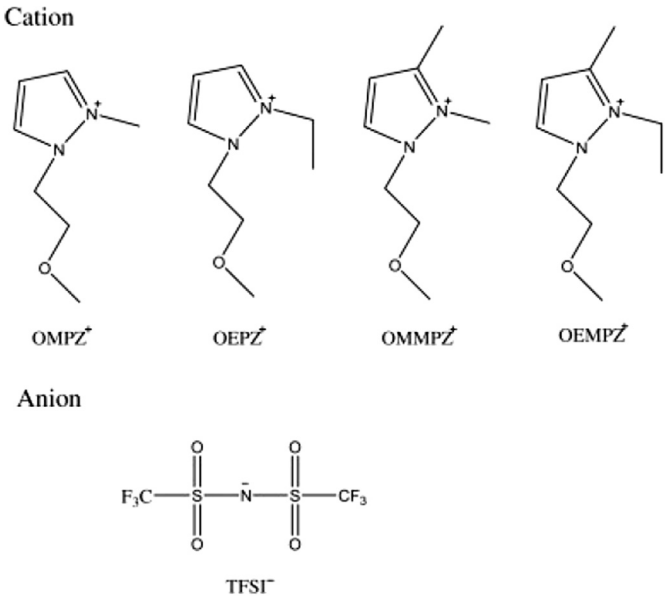

Fig. 9. Structures of cations and anion of the four pyrazolium based ILs. Copyright 2011 Elsevier.

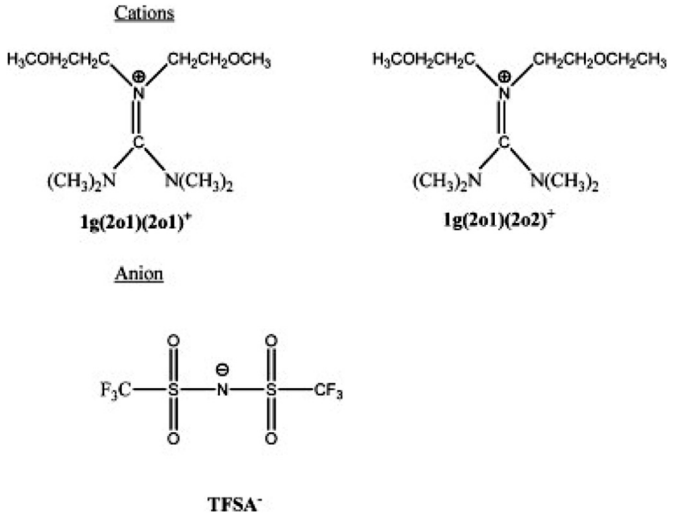

Fig. 10. Structures of cations and anion of the guanidinium based ILs. Copyright 2011 Elsevier.

Recently, a new class of ionogel electrolyte for lithium-ion batteries was reported, which can be prepared in either "liquid-in-solid" or "solid-in-liquid" form. The electrolytes are prepared by a non-aqueous self-assembly sol–gel process, in which ionic liquid electrolyte is immobilized within an inorganic gel. The inorganic gels weaken the interaction of anions and cations and thereby improve lithium salt dissociation and enhance transport of Li^+ [68].

4.2. ILs as electrolytes for Li–S and Li-Air batteries

The first paper reporting ILs as the electrolyte for Li–S batteries appeared in 2006 which exhibited some interesting improvements [69]. IL based electrolytes can reduce the shuttle mechanism because that ILs have high viscosity and low solubility of Li polysulfides. Byon et al. [70] reported about DME with *N*-methyl-*N*-propylpiperidinium bis-(trifluoromethanesulfonyl) imide (PP_{13}TFSI) together as electrolyte for Li–S batteries. In this electrolyte, PP_{13}–TFSI decreased the solubility and diffusion rate of Li polysulfides while DME had reverse effect in order to get a balance. Results exhibited a discharge capacity of about 1360 mAh g^{-1} at 0.1 C, much better than the neat PP_{13}–TFSI or DME-based electrolyte. It suggests that the IL combined with organic solvents as electrolyte will have better property of electrochemistry. Recently, Wang et al. [71] used PP_{13}TFSI as electrolyte working in combination with $LiNO_3$, zero self-discharge can be achieved to rest a full-charged Li–S cell for two days.

Li-air batteries using ILs as electrolytes have several advantages over traditional non-aqueous electrolytes due to the ultralow vapor pressure and hydrophobic property of ILs. However, the research on this field just starts. Kuboki et al. [72] reported the first paper about Li–air battery based on ILs. Mizuno et al. [73] have showed that *N*-methyl-*N*-propylpiperidinium bis (trifluoromethanesulfonyl) amide (PP_{13}–TFSI) which has less positive atomic charge was more stable than carbonate solvents. Recently, a Li–air battery using PYR_{14}TFSI–LiTFSI as ILs electrolyte was reported [74]. The energy efficiency showed an apparent improvement to 82%, when the charge process was at a very low overvoltage.

5. Polymer electrolytes

Polymer electrolytes provide a possible solution to overcome the low mechanical strength and safety issue of liquid electrolytes. According to the material state, polymer electrolytes could be classified into solid polymer electrolytes and gel polymer electrolyte. Solid polymers have better mechanical properties than gel polymer, and both of them are generally more beneficial than liquid electrolytes in terms of the safe use of batteries. Details will be further discussed in the following part.

5.1. Solid polymer electrolytes

Poly(ethylene oxide) (PEO) is the most common polymer electrolytes. PEO was found to be conductive when complexed with an alkali metal ion in 1973. After that, PEO was used as electrolytes for battery in 1979 [75]. Solid polymer electrolytes have many advantages including dimensional stability, safety and the ability to prevent lithium dendrite growth. However, the low ionic conductivity limits its application and several measurements have been taken to solve this problem.

Adding lithium salts to solid polymer electrolytes can improve the ionic conductivity effectively. Lithium trifluoromethanesulfonate (LiTf), lithium bis(trifluoromethanesulfonimidate) (LiTFSI), lithium bis(trifluoromethanesulfonimide) (LiBETI), lithium perchlorate ($LiClO_4$) and lithium bis(oxalato)borate (LiBOB) have been used to improve the ionic conductivity [76], but none of these lithium salts have a significant improvement in the electrolyte, almost below 10^{-4} S cm^{-1} at room temperature [77]. Recently, Yang et al. reported a PEO/Li^+ solid polymer electrolyte synthesized by the supramolecular self-assembly of PEO, α-cyclodextrin (α-CD), and $LiAsF_6$. Such electrolytes have high ionic conductivity because Lithium ions can transfer in nanochannels and different charge ions are separated. They facilitate the lithium ions transportation by increasing the cavity size of the channel, so that the conductivity can be improved [78].

The addition of ceramic particles, such as SiO_2, Al_2O_3, Fe_3O_4, TiO_2 and S–ZrO_2, to polymer electrolytes also leads to an increase in conductivity, mechanical and electrochemical properties [75]. The poly(methacrylate) (PMA)/poly(ethylene glycol) (PEG)-$LiClO_4$-3 wt% SiO_2 polymer electrolyte exhibited an optimum ionic conductivity of 0.26 mS cm^{-1} at room temperature [79]. Liu et al. reported a novel ceramic material which prepared $Li_{0.33}La_{0.557}TiO_3$ nanowires by electrospinning and then synthesized a polyacrylonitrile-$LiClO_4$ incorporated with 15 wt% $Li_{0.33}La_{0.557}TiO_3$ nanowire composite electrolyte, which exhibited an ionic conductivity of 2.4×10^{-4} S cm^{-1} at room temperature [80]. Carbon

nanotubes have also been used as an additive for solid polymer electrolytes and packaged within insulating clay layers so that they cannot cause the electrical shorting. This kind of polymer electrolyte can not only increase the lithium ion conductivity, but also improve the mechanical properties [81].

There are many novel solid polymer electrolytes. Single-ion conducting solid polymer electrolytes have been used to eliminate the concentration polarization at electrode interfaces, but most of these electrolytes are characterized with low ionic conductivities [77]. Bouchet et al. [82] reported the single-ion BAB triblock copolymer electrolytes with a well performance, the ionic conductivity being 1.3×10^{-5} S cm^{-1} at 60 °C, the lithium transfer number over 0.85, the improved mechanical strength to 10 MPa at 40 °C, and the electrochemical stability window up to 5 V *vs.* Li^+/Li. Recently, Lu et al. found that the cell with nanoporous − lithiated perfluorinated polymer single-ion electrolyte membrane is able to cycle reversibly for more than 1960 h of continuous charge−discharge operation, because of its remarkable ability to stabilize lithium electrodeposition and stop dendrite growth in lithium battery [83]. Poly(ionic liquid)s (PILs) is a new type of polymer. Zhang et al. designed a class of PILs with ionic conductivity of 5.32×10^{-3} S cm^{-1} at room temperature and electrochemical stability window above 5 V *vs.* Li^+/Li [84].

An innovative polymer electrolyte system by regulating the mobility of classic −EO− based backbones was reported recently [85]. Room temperature ionic conductivity values (>0.1 mS cm^{-1}) were observed, with an electrochemical stability window (>5 V *vs.* Li/Li^+) and excellent lithium ion transference number (>0.6). Moreover, the efficacious resistance to lithium dendrite nucleation and growth make the implementation of these polymer electrolytes promising in next generation of all-solid Li-metal batteries.

5.2. Gel polymer electrolytes

Compared with solid polymer electrolytes, polymer gel electrolytes (GPEs) are more practical [77]. GPEs have attracted particular attention due to their low volatility, high thermal stability and safety [86]. Poly(vinylidenefluoride) (PVdF) is the most commonly polymer gel electrolytes, due to the strongly electron-withdrawing functional group (−C−F), PVdF-based polymer electrolytes can be highly anodic stable. Besides, high dielectric constant ($\varepsilon = 8.4$) of PVdF can assist in greater ionization of lithium salts, so that provide a high concentration of charge carriers [87]. The first commercial GPE cell was based on PVdF-hexafluoropropylene (HFP) copolymer electrolyte [7]. Zhang et al. [88] reported PVdF-HFP membranes with honeycomb-like porous architectures, which leads to the electrolyte uptake of 86.2%, show the ionic conductivity of 1.03 mS cm^{-1} at room temperature, a high thermally stability up to 350 °C and fire-proof capability, the electrochemistry stability is up to 5 V. The electrochemical performance has also been tested. They believed that the performance is related to the multi-sizes porous structure. Oligomeric ionic liquid (OIL) was used to synthesized a PVdF-HFP based GPEs, due to the existence of the oligomeric ionic liquid, the GPE dimensional stability has been improved at high temperature, the electrolyte's limiting oxygen index is 29 means it is flame-retardant under a normal atmosphere [89].

It is known that the poor mechanical property limit the application of GPEs, so improvement of the mechanical strength is important. Zhu et al. [90] prepared a PVdF-glass fiber mats (GFM) composite membrane, which show an acceptable mechanical property, the maximums stress and strain are 14.3 MPa and 1.8%. Electrospun PVdF was also used to form a membrane. Zhu et al. [91] used the single-ion conductor (lithiumpolyvinyl alcohol oxalate borate (LiPVAOB)) and electrospun PVdF to prepared a composite membrane, the mechanical property is much higher than that of PVdF-GFM membrane, the maximal stress and strain are 32.4 MPa and 3.1%. The good mechanical property of PVdF-LiPVAOB owing to the existence of electrospun PVdF has been proved by FT-IR detection.

Besides poor mechanical strength, low interfacial stability toward lithium metal is another critical issue of the PVdF-based polymer electrolytes [87]. Kuo et al. [89] found that high OIL content PVdF-HFP/OIL GPE has a lower interfacial resistance and strongly mitigates the increase in cell impedance, which means the interface is more stable when the content of OIL is high. OIL enhanced the interfacial stability mainly due to the ease of ion transportation. The lithium salt significantly affects the interfacial resistance, because it can affects the reaction of the electrolyte with the electrode. The initial interfacial resistance of PGE follows the order $LiBF_4$ (48.7) < LiTFSI (73) < $LiCF_3SO_3$ (99.8) < $LiClO_4$ (106) < $LiPF_6$ (122 Ω), after storage, the interfacial resistance for all PGEs will increase as shown in Fig. 11, after a period of storage of 12 days the interfacial resistance values (Ω) follows the order $LiBF_4$ (85) < LiTFSI (115) < $LiClO_4$ (149) < $LiCF_3SO_3$ (186) < $LiPF_6$ (215) [92]. The passivation layer on the lithium electrode surface and degradation of

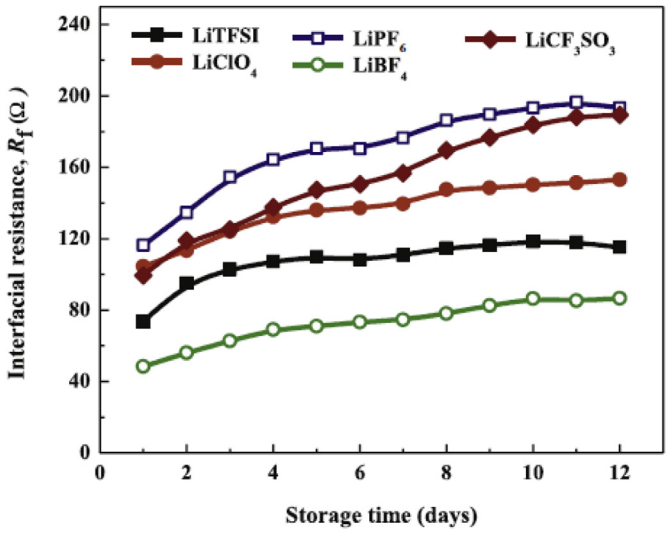

Fig. 11. Time dependant interfacial behaviors for PGE based on electrospun PVdF/PEO polymer blend membrane with different electrolytes (Li/PGE/Li cell, frequency range 10 mHz−1 MHz). Copyright 2014 Elsevier.

physical can tact between the electrode and PGE maybe cause the increase in interfacial resistance with storage. So the interfacial stability of electrode and PGE still need to be investigated.

Poly(methyl methacrylate) (PMMA) and poly(acrylonitrile) (PAN) also can be used to prepared GPEs. PMMA has been added to PVdF to improve the electrolyte performance [93,94]. The addition of PMMA increased the pore size, porosity and electrolyte uptake of the PVdF membrane, which in turn increased the ionic conductivity of the polymer electrolyte. The degree of crystallinity of a polymer blend membrane decreases as the PMMA concentration increases [93]. Prasanth et al. [95] reported a polymer blend of PAN/PMMA/polystyrene(PS) electrolyte for lithium ion batteries, which have a thermal stability up to 295 ± 5 °C, the ionic conductivity of about 3.9×10^{-3} S cm^{-1}. PMMA-based GPEs also have been applied in Li–air battery, due to the absence of the blocked pores caused by the flooding liquid electrolyte and enhancement of the oxygen diffusion in cathode, the PMMA-based Li–O_2 battery show an enhanced cyclic stability [96]. PMMA based GPEs satisfy the basic need of electrolyte, but the poor mechanical property limits their application.

PAN possesses good mechanical strength, heat resistance, chemical stability and good flame retardancy, but the interface stability is poor. In order to overcome the short slab of single polymer, a core–shell structure GPE has been prepared [97,98]. The core–shell structure polymer nanofiber has been synthesized by coaxial electrospinning, show excellent interface stability [97]. The microstructure, crystallinity, thermal stability and mechanical properties of nanofiber membranes could be adjusted by changing the concentration of core–shell spinning solution [98].

As a low molecular weight polyether, poly(ethylene glycol) (PEG) has a good solvating ability of Li^+, Huang et al. [99] reported a poly(methacrylate) (PMA)/PEG-based GPE with $LiClO_4$/DMSO loading and Calix[4]quinone (C4Q) Cathode lithium ion batteries. A capacity of 380 mAh g^{-1} has been maintained after 100 cycles at a 0.2 C charge/discharge rate, show a desirable electrochemical performance.

6. Hybrid electrolytes

Ionic liquid and polymer show a series of advantages to be electrolytes as mentioned in the above sections, but they still have some weaknesses. Ionic liquid show poor mechanical performance, low lithium ion transference numbers and failure to prevent lithium dendrite growth in lithium metal battery. Polymer has a low ionic conductivity, low mechanical properties and narrow electrochemical stability window. Besides, partial delamination of Li foils and the polymer/solid electrolyte layers is also responsible for capacity fade and failure. A novel kind of electrolyte, hybrid electrolyte, has been synthesized to overcome the shortage of ionic liquid and polymer electrolyte. Hybrid electrolytes of lithium battery could be roughly divided into two major classifications: one is based on ionic liquid, the other is based on polymer, and both of them will be introduced in this section.

6.1. Ionic liquid-nanoparticle hybrid

Different kinds of nanoparticles have been used to synthesize ionic liquid-nanoparticle hybrid electrolytes, such as ZrO_2 [100], TiO_2 [101] and SiO_2 [102]. The IL-ZrO_2 hybrid electrolytes show tunable mechanical properties and excellent interfacial stability. The lithium transference number of such electrolyte is up to 0.35 ± 0.04, seven times higher than that of pure IL electrolytes, because the tethering of the IL cation makes Li^+ the only mobile cation [100].

Lu et al. [103–106] conducted a series of studies on ionic liquid nanoparticle hybrid electrolytes, the structure of these hybrid electrolytes have been shown in Fig. 12 [105], which tether ionic liquid to silica nanoparticle. They measured several properties of these electrolytes and tested the electrochemistry performance in secondary lithium metal batteries. Ionic conductivity in the range of $10^{-2} - 10^{-4}$ S cm^{-1} at room temperature is the common characteristic of these electrolytes. The electrochemical stability windows are around 4 V *vs.* Li/Li^+. The SiO_2-IL-TFSI/LiTFSI hybrid also possesses a high thermally stability (400 °C) and high shear mechanical moduli (10^5–10^6 Pa). The authors found that lithium transference numbers are increased with particle, at a particle loading of 48 vol% and the lithium transference number of SiO_2-piperidinium ILs-TFSI hybrid electrolytes up to 0.22 [103]. The short circuit time of lithium metal battery based on ionic liquid-nanoparticle hybrid electrolytes is an order of magnitude higher than that of the pure PC, which indicates that ionic liquid-nanoparticle hybrid electrolytes can effectively retard the growth of lithium dendrites. They put forward two mechanisms for retarding lithium dendrites [105]. One is to decrease the space charge, because it causes uneven lithium deposition at high current density. Nanoparticles can prevent space charge by adjusting the anion concentration. Another reason is that the hybrid electrolytes are difficult to across. Because of the strong mechanical properties and highly tortuous path, the nucleated dendrites are hard to short-circuit the cell [106].

6.2. Polymer based hybrid electrolyte

Polymer based hybrid electrolyte is also a kind of attractive electrolyte. The majority of these electrolytes are composed of organic and inorganic materials, usually using SiO_2, TiO_2

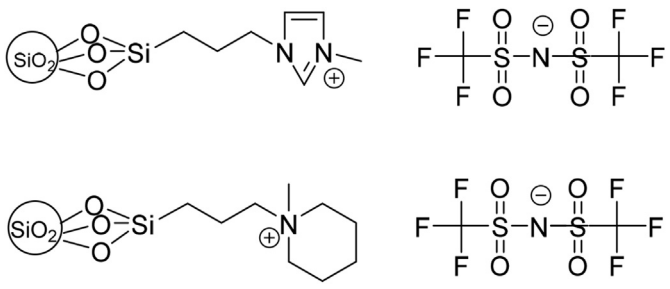

Fig. 12. Structure of ionic liquid-nanoparticle hybrid electrolytes. Copyright 2014 Wiley-VCH Verlag GmbH & Co. KGaA, Weinheim.

nanoparticle or polyhedraloligomeric silsesquioxane (POSS) as the inorganic part, and polymer as the organic part. Compared with polymer electrolytes, polymer-based hybrid electrolytes overcome several weaknesses, such as low mechanical properties, narrow electrochemical stability windows and low ionic conductivity.

Polymer-based hybrid electrolyte is usually synthesized by sol–gel method. Kao and Chen [107] reported a new way to synthesis organic–inorganic hybrid electrolyte, which derived from the self-assembly of a PEO–PPO–PEO triblock copolymer by co-condensation of (3-glydicyloxypropyl) trimethoxysilane and tetraethoxysilane. This kind of electrolytes can be a substantial suppression of polymer crystallization. Kao's work was successful in preventing polymer crystallization, but failed to characterize the mechanical properties. It is known that POSS can improve the mechanical strength of polymers, and several polymer-based electrolytes use it as the inorganic part [108,109]. Pan et al. reported a POSS–PEG hybrid electrolyte and measured the mechanical properties by dynamic mechanical analysis (DMA) [109]. Besides mechanical properties, they found the ability of ionic conductivity and resistance to lithium dendrite growth can also be adjusted by changing the cross-linked structures. The ion conductivity at room temperature can reach ~0.1 mS cm^{-1}. The size of nanoparticle will influence the conductivity, when the volume of small and large particles is the same. The conductivity of hybrid electrolyte is ten-times larger than that of the pure small or large particles [110].

SiO_2-polymer hybrid electrolyte was created by dense functionalization of SiO_2 nanoparticles with short polymer chains. These electrolytes show superionic conductivities, large electrochemical stability windows (−0.5 V to >5 V, *vs.* Li), typical lithium ion transference numbers (~0.1–0.25), no volatility, thermal stabilities up to 400 °C and high mechanical properties [111]. By means of adjusting the volume fraction of the inorganic component, the mechanical properties of the electrolyte can be tuned [111,112].

Recently, Choudhury et al. [113] reported crosslinked polymer-nanoparticle composite (CNPC) electrolytes, which combine the best performance of solid polymers, nanocomposites and gel-polymer electrolytes. The highly crosslinked structure makes it possible to show both high mechanical strength (G_N = 1 MPa) and high ionic conductivity (σ_o = 5 mS cm^{-1}) at room temperature. Besides, it can also suppress the growth of dendrite, and the short circuit time is higher. CNPC membranes were soaked in the EC/DEC (1v:1v) electrolyte solvent mixture containing 1 M LiPF6 salt, then a cell with metallic lithium as anode, lithium titanium oxide (LTO) as cathode, CNPC + EC:DEC (1 M $LiPF_6$) as electrolyte was prepared. Li | CNPC + EC:DEC (1 M $LiPF_6$) | LTO cells have a high current densities at a current density of 0.5 mA cm^{-2}. The batteries retain high capacity for at least 150 cycles at high current densities, as shown in Fig. 13 [113]. The CNPC electrolyte also shows a high stability window, with cathodic stability of at least 5 V *vs.* Li^+/Li and a coulombic efficiency nearing 100%.

7. Electrolytes for beyond Li-based batteries

Rechargeable Li-based batteries have been extensively investigated due to their excellent energy and power density. However, their disadvantages including cost, lithium resource, reliability, and safety are obvious. For example, the relative abundance of different elements in the Earth's crust is shown in Fig. 14 [114]. The relative abundance of lithium in the Earth's crust is limited to be only 20 ppm. Indeed, the materials cost (the price of Li_2CoO_2) was steeply increased during the first decade of this century. In order to address the above issues, some studies on rechargeable batteries have focused on exploring host materials that can reversibly accommodate and release guest ions alternative to Li^+, such as monovalent H^+, Na^+ and K^+ and multivalent Mg^{2+}, Ca^{2+}, Zn^{2+}, and Al^{3+} cations. It is generally accepted that the electrochemical properties of host materials can vary with different guest ion

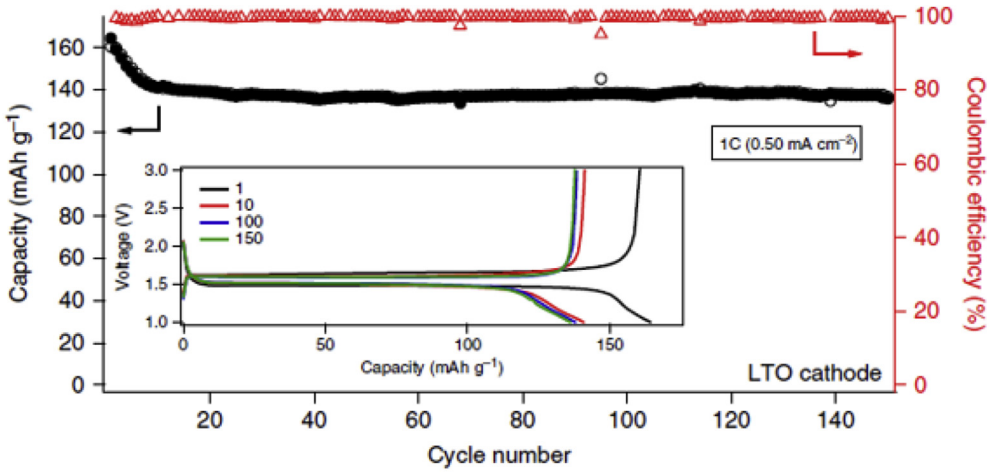

Fig. 13. Cycling performance for Li | CNPC + EC:DEC (1 M $LiPF_6$) | LTO at 1 C (0.50 mA cm^{-2}). The inset shows the voltage profiles of the same. Copyright 2015 Macmillan Publishers Limited.

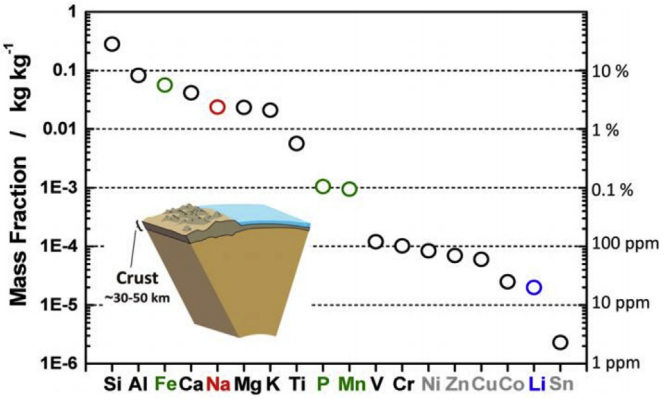

Fig. 14. Elemental abundance in the earth's crust. Copyright 2014 American Chemical Society.

species in terms of cycle stability, rate capability, and energy density [115]. Early studies have examined monovalent ion host materials, such as H^+ and K^+ insertion materials. Among them, various metal–organic frameworks (MOFs) and oxide based electrode materials showed reversible electrochemical activity with H^+ and K^+ [115]. In this section, we mainly focus on the development of electrolytes in Na-, Mg-, Ca-, Zn- and Al-based batteries, H- and K-electrochemistry are not in this scope.

7.1. Na-based batteries

Owing to the low cost and high natural abundance of sodium, rechargeable Na batteries (such as Na-ion, Na-air/$Na-O_2$, Na–S, and $Na-NiCl_2$ (ZEBRA) batteries) have been investigated as a potential alternative to Li-based batteries [116–128]. Many of the electrolytes used in the state of the art Li batteries are in general valid also for Na-based batteries due to the chemical similarity between the Na and Li elements. Generally, the electrolytes of interest for Na batteries can be classified into 1) aqueous solution; 2) non-aqueous organic electrolyte consisting of a sodium salt solubilized in an organic solvent or solvent mixture; 3) ionic liquid consisting of an organic salt (R^+X^-) doped with a fraction of the sodium salt equivalent (Na^+X^-) and 4) solid state electrolytes.

7.1.1. Aqueous electrolytes

Rechargeable sodium batteries can be more cost-effective in aqueous systems because the water and Na salts such as Na_2SO_4, NaCl, and $NaNO_3$ are inexpensive due to their natural abundance. Besides, they are environmentally benign, have high ionic conductivities and can achieve higher power than organic electrolytes. However, electrode materials for aqueous rechargeable sodium batteries (ARSBs) should satisfy several conditions for use in aqueous electrolytes. First, the electrode redox potentials should be located between those of O_2 and H_2 evolution to avoid water splitting during electrochemical cycling (2.297 and 3.527 V *vs.* Na^+/Na at neutral pH). As shown in Fig. 15, the potential range is dependent on the pH of the aqueous solution. Second, the electrode needs to be chemically stable at the operating pH of the electrolyte. Dissolution of materials and side reactions in the presence of O_2 should not occur. Residual O_2 can cause side reactions of Na-intercalated + $1/2H_2O$ + $1/4O_2$ → Na^+ + OH^-, which can occur at comparably high voltages. Third, the Na-containing electrode materials should be used as a cathode for ARSBs. Otherwise, the presodiated anode material should be used to make the system work. Additionally, an open framework structure suitable for large ion insertion with low volume expansion is preferable, as is also required for conventional sodium ion batteries [115]. Various aqueous solutions have been evaluated for their use in ARSBs as shown in Table 2.

The main disadvantage of aqueous electrolytes is the relatively low decomposition voltage, theoretically only 1.23 V.

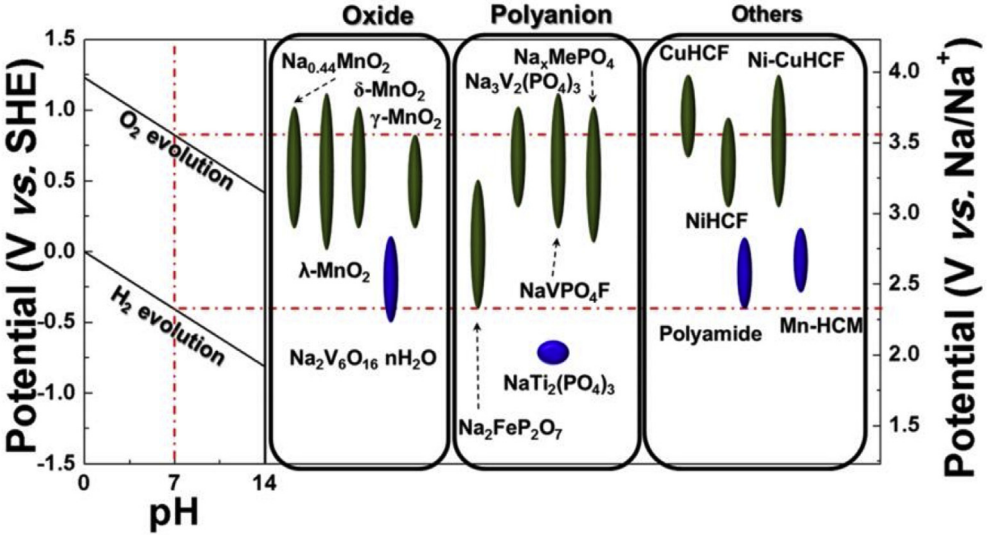

Fig. 15. Electrode materials for aqueous rechargeable sodium batteries (ARSB). The potentials of the electrode materials are described *vs.* SHE and Na^+/Na. The red dotted line illustrates H_2 and O_2 evolution limits in a neutral aqueous solution. Copyright 2014 American Chemical Society.

Table 2
Some of the aqueous solutions used in Na-based batteries.

Salt	pH	Concentration	Active materials	Ref.
Na_2SO_4	Neutral	1, 2 M	$NaTi_2(PO_4)_3$	[129,130]
Na_2SO_4	7–8	1 M	$Na_{0.44}MnO_2$	[131,132]
Na_2SO_4	Neutral	1 M	$Na_2FeP_2O_7$	[133]
Na_2SO_4	Neutral	1 M	Na_2NiHCF	[134]
Na_2SO_3	Neutral	0.5 M	C–$LiTi_2(PO_4)_3$	[135]
$NaNO_3$	Neutral	1 M	$CuxNi_{1-x}HCF$	[136]
$NaNO_3$	Neutral	1 M	$Na_{0.44}MnO_2$	[137]
$NaNO_3$	Neutral	5 M	Polyimide	[138]
NaOH	Alkaline	7 M	MnO_2	[139]
NaOH	Alkaline	7 M	$NaMn_{1/3}Co_{1/3}Ni_{1/3}PO_4$	[140]
NaOH	Alkaline	2 M	$NaMn_{1/3}Ni_{1/3}Co_{1/3}PO_4$	[141]

Using electrode materials of high hydrogen and oxygen overvoltage, battery voltages up to 2 V are possible, as in the case of lead–acid batteries. However, all aqueous electrolyte battery systems with voltages above 1.23 V are from the thermodynamic point of view unstable and will therefore have a certain rate of self-discharge [142]. There are a few possible approaches to these strategies: 1) application of more than one type of electrolyte in a single system to utilize alkali-metal anodes with low redox potential, 2) construction of rechargeable metal–air batteries with high storage capacity, and 3) utilization of aqueous-type cathodes with reversible redox reactions, resulting in a flexible capacity.

7.1.2. Non-aqueous organic electrolytes

The most common electrolyte formulation for rechargeable sodium batteries is a sodium salt dissolved in an organic solvent such as carbonate, ester, and ether or the solvent mixture. Parameters affecting the choice of sodium salts and organic solvents are the same or similar for rechargeable sodium and lithium battery electrolytes. Some of non-aqueous organic electrolytes used in sodium batteries are listed in Table 3.

The same prospective anions as applied in electrolytes of rechargeable lithium batteries such as ClO_4^-, BF_4^-, PF_6^-, $CF_3SO_3^-$(OTf), and $[N(CF_3SO_2)_2]^-$ (TFSI) are found for rechargeable sodium battery electrolytes. The promises and drawbacks of the above anions are more or less the very same with those in Li electrochemistry, since many properties are more often dependent on the anion than on the cation [177]. While being only of academic interest, the most commonly used salt (in ~2/3 of the published papers of sodium batteries) is $NaClO_4$, which is likely due to a combination of historical and cost reasons. The second most popular salt is indeed $NaPF_6$, which enables comparisons with many rechargeable lithium batteries studies.

In search of suitable sodium salts for electrolytes of rechargeable sodium batteries, Bhide et al. [152] examined the properties of $NaPF_6$, $NaClO_4$ and NaOTfin a binary mixture solvent of ethylene carbonate (EC) and dimethyl carbonate (DMC) (30:70 wt%) for sodium ion batteries (SIBs). It is well known that the conductivity of the electrolytes is determined both by the salt concentration and the temperature. They found that the electrolytes containing 0.6 M $NaPF_6$ (6.8 mS cm^{-1}) and 1.0 M $NaClO_4$ (5.0 mS cm^{-1}) have the most promising conduction characteristics at room temperature. However, the conductivity of NaOTf is much smaller (3.7 mS cm^{-1}, 0.8 M) than the other two. The electrochemical stability window of the different electrolytes was studied by linear sweep voltammetry (LSV) and cyclic voltammetry (CV) measurements with respect to a variety of working electrodes (WE) such as glassy carbon (GC), graphite and a carbon gas diffusion layer (GDL). Electrolytes containing $NaPF_6$ and $NaClO_4$ were found to be electrochemically stable with respect to GC and GDL electrodes up to 4.5 V *vs.* Na/Na^+, while some side reactions starting from around 3.0 V for the latter salt. The results also indicated that aluminum is preferred over different steels as a cathode current collector and copper is stable up to a potential of 3.5 V *vs.* Na/Na^+. Coupled with $Na_{0.7}CoO_2$ as a positive electrode, the electrochemically properties of the electrolytes were investigated. It is indicated that the electrolyte $NaPF_6$ in EC:DMC is favorable for the formation of a stable surface film and the reversibility of the above cathode material.

A much more exhaustive investigation on electrolyte solvents (PC, EC, DMC, DME, DEC, THF and Triglyme) or solvent mixtures (EC:DMC, EC:DME, EC:PC and EC:Triglyme) and solutes($NaClO_4$, $NaPF_6$ and NaTFSI) was carried out by Ponrouch et al., who characterized the Na^+ transport, viscosity, thermal stability, service temperature range, and electrochemical stability window as well as cycling performance of numerous mixtures of carbonate esters and ethers [143,178]. The conductivity values for PC-based electrolytes (Fig. 16a) are relatively similar, ranging from 7.98 for $NaPF_6$ to 6.2 mS cm^{-1} for NaTFSI and being intermediate for $NaClO_4$. In contrast, larger ionic conductivity variations were found by fixing the salt ($NaClO_4$) and changing the nature of the solvents with σ values following the trend EC:DME > EC:DMC > EC:PC > EC:Triglyme > EC:DEC > PC > Triglyme>>> DME, DMC, DEC (Fig. 16b). Electrochemical tests were then performed using three-electrode Swagelok cells with Na as counter and reference electrodes. When dealing with the single solvent based electrolytes with 1 M $NaClO_4$, the electrochemical stability decreases following the trend DEC > PC > Triglyme > DME > DMC > THF. Under similar experimental conditions, the electrochemical stability of binary solvent-based electrolytes decreases following the trend
EC:PC > EC:DMC > EC:DME > EC:DEC > EC:Triglyme. The electrochemical stability window was further studied by performing electrochemical impendence spectroscopy (EIS) measurements. Similar trends as the CV results are observed for all electrolytes tested as shown in Fig. 17. Cells were then assembled using these electrolytes and hard carbon negative electrodes. Their electrochemical performance was found to be remarkably dependent on the electrolyte solvent used, EC:PC emerging as clearly optimum. On the other hand, no significant differences were observed when using $NaClO_4$ or $NaPF_6$ as the electrolyte salt.

Recently, new salts such as borates (NaBOB, NaBSB, NaBDSB, NaDFOB, etc.) and heterocyclic anions (NaTDI, NaPDI, etc.) were also evaluated for sodium-based batteries

Table 3
Some of non-aqueous organic electrolytes used in sodium-based batteries.

Salt	T_m (°C)	σ (mS cm^{-1})	Solvent	Concentration	Electroactive materials	Ref.
$NaClO_4$	468	6.4	PC	1 M	Hard carbon $NaMF_3$ $NaMPO_4F$ $NaCoO_2$ $Na_xFe_{0.5}Mn_{0.5}O_2$ $NaCrO_2$	[143–148]
		–	EC	1 M	Carbon fiber Hard carbon	[149,150]
		–	EC:PC	1 M	Hard carbon $NaFePO_4$ $NaNi_{1/3}Mn_{1/3}Co_{1/3}O_2$	[139,143,151]
		5.0	EC:DMC	1 M	$Na_{0.7}CoO_2$ Petroleum coke $NaxMnO_2$ $NaVPO_4F$ Carbon black Carbon microspheres $NaV_{1-x}Cr_xPO_4F$	[152–158]
		–	EC:DEC	1 M	NaV_6O_{15} Hard carbon	[159,160]
$NaPF_6$	300	7.98	PC	1 M	Hard carbon Na_xFePO_4F	[143,161]
		–	DME	1 M	$NaCoO_2$	[162]
		6.8	EC:DMC	0.6 M 1 M	$Na_{0.7}CoO_2$ Petroleum coke Porous carbon	[152,153,163]
		–	EC:DEC	1 M	Na_xFePO_4F Nanoporous carbon Na–Sn	[161,164,165]
NaOTf	248	3.7	EC:DMC	0.8 M	$Na_{0.7}CoO_2$	[152]
		–	Tetraglyme	1 M	Na–S battery	[166]
		–	Diglyme	1 M	Na–O battery	[167,168]
		–	DOL:DME	1 M	Na–S battery	[169]
NaTFSI	257	6.2	PC	1 M	$NaCrO_2$	[143,170]
NaTDI	>330	4	PC	1 M	–	[171]
NaFSI	118	–	PC	1 M	$NaFe_x(Ni_{0.5}Ti_{0.5})_{1-x}O_2$ $Na_2Ti_3O_7$	[172–174]
NaBOB NaBSB NaBDSB	–	0.071–0.256 0.258–1.548 1.111–0.974 0.160–0.599 0.60–0.501	PC AN DMF PC + AN PC + DMF	0.025 M	–	[175]
NaDFOB	–	4.27 5.32 7.74 5.36	PC EC:DEC EC:DMC EC:PC	1 M	$Na_{0.44}MnO_2$	[176]

[171,175,176]. A new electrolyte salt, sodium-difluoro(oxalato)borate (NaDFOB), was synthesized and studied by Chen et al. [176] They found that NaDFOB has excellent compatibility with various common solvents used in Na-ion batteries, in strong contrast to the solvent dependent performances of $NaClO_4$ and $NaPF_6$. In addition, NaDFOB possesses good stability and generates no toxic or dangerous products when exposed to air and water. Plewa-Marczewska et al. synthesized two imidazole fluorine derivative sodium salts: sodium 4,5-dicyano-2-(trifluoromethyl)imidazolate (NaTDI) and sodium 4,5-dicyano-2-(pentafluoroethyl)imidazolate (NaPDI) for application in liquid nonaqueous sodium electrolytes [171]. NaTDI and NaPDI based electrolytes in PC show good conductivity with the values about 4 mS cm^{-1} at 20 °C for salt concentration 0.5 and 1 M for each salt. However, electrochemical performance of NaTDI and NaPDI in practical Na ion batteries has not been carried out yet.

7.1.3. Ionic liquid

Ionic liquids (ILs) have many properties of interest for safer and in some cases environmentally friendly batteries, such as non-volatility and non-flammability. However, studies of ILs containing a fraction of sodium salts to create rechargeable sodium battery electrolytes are still at a very early stage. There are only a few reports on the study of electrode materials in ILs [179,180]. Ding et al. report the electrochemical

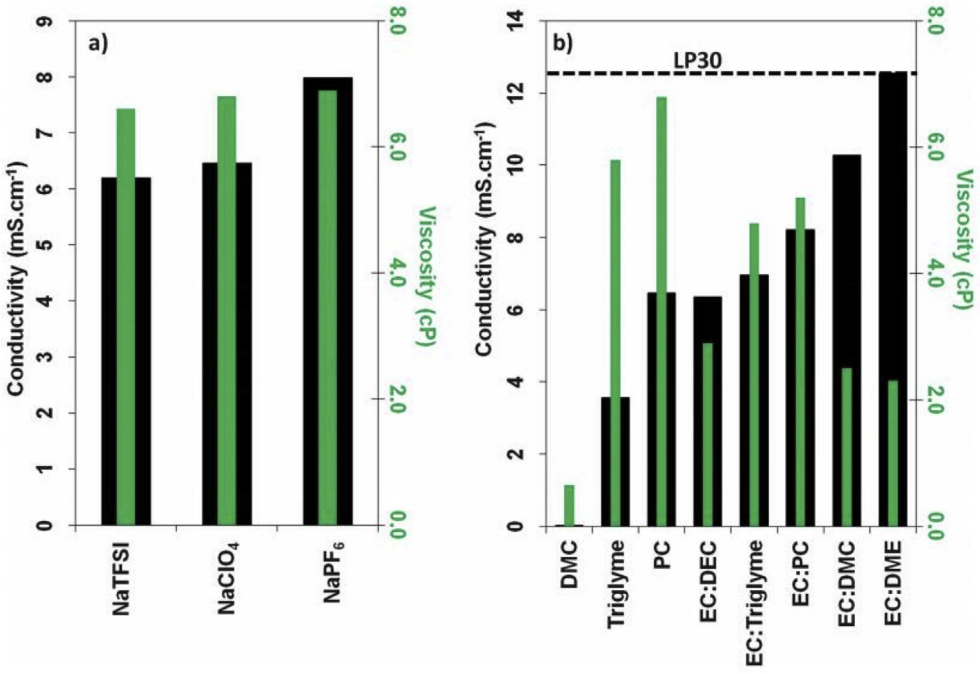

Fig. 16. Conductivity (black bars and left hand side *y* axis) and viscosity (green bars and right hand side *y* axis) values of (a) PC based electrolytes with 1 M of various Na salts and (b) electrolytes based on 1 M $NaClO_4$ dissolved in various solvents and solvent mixtures. Copyright 2012 The Royal Society of Chemistry.

performance of a hard carbon (HC) negative electrode in Na[FSA]-[C_3Clpyrr][FSA] (FSA = bis(fluorosulfonyl)amide, C_3Clpyrr = *N*-methyl-*N*-propylpyrrolidinium) IL over a wide temperature range of 10–90 °C [180]. Surprisingly stable cyclability is observed for the HC electrode at 90 °C, *i.e.* a capacity retention ratio of 84% after 500 cycles. Finally, a high full-cell voltage of 2.8 V and stable full-cell operation with Coulombic efficiency higher than 99% are achieved for the

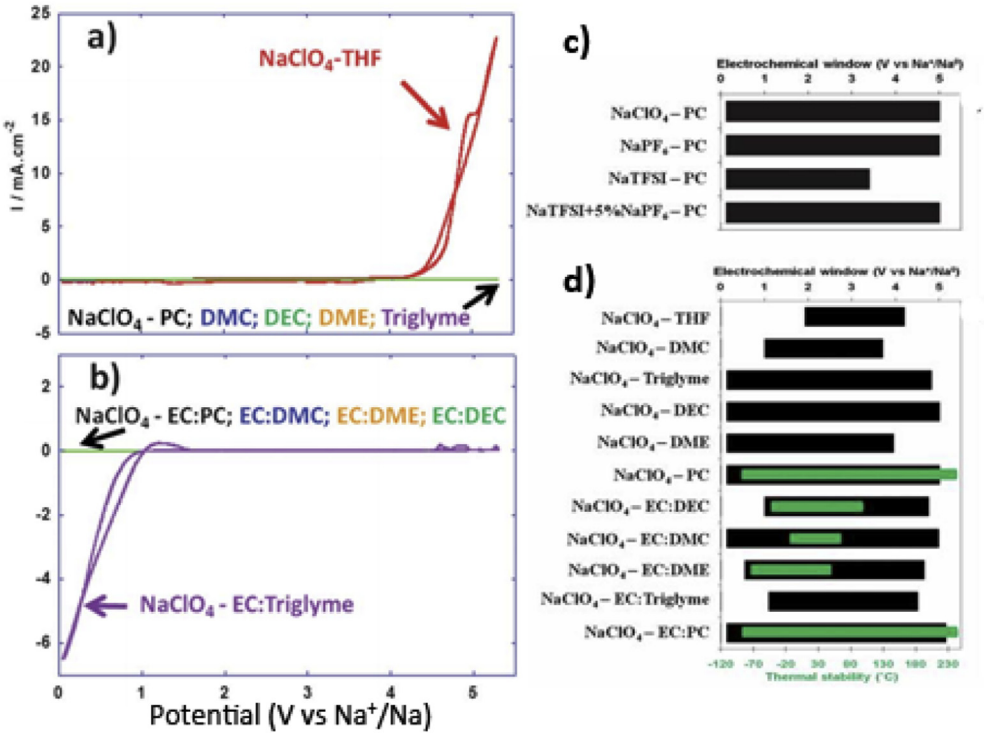

Fig. 17. CVs (10 mV s^{-1}, high purity Al plungers) obtained in three-electrode Swagelok cells with (a) 1 M $NaClO_4$ dissolved in single solvents, (b) 1 M $NaClO_4$ dissolved in solvent mixtures. Electrochemical potential window stability (black bars and upper y axis) and thermal range (green bars and lower *y* axis) values of (c) PC-based electrolytes with 1 M of various Na salts and (d) electrolytes based on 1 M $NaClO_4$ dissolved in various solvents and solvent mixtures. Copyright 2012 The Royal Society of Chemistry.

first time when using $NaCrO_2$ as the positive electrode at 90 °C.

ILs such as 1-butyl(propyl)-1-methylpyrrolidinium bis(trifluoromethylsulfonyl)imide ([C4(C3)mpyr]-[TFSI]) doped with NaTFSI are able to reversibly strip and deposit sodium at room temperature [181–183]. A moderate overpotential of only 0.2 V for sodium electrodeposition was measured at room temperature; traces of water in the electrolyte were detrimental. A voltage window of 5.2 V versus Na/Na^+ was reported together with good compatibility with the layered oxide cathode material $NaCrO_2$ [183]. Compatibility of the polyanion cathode material $NaFePO_4$ with the NaTFSI-doped [C4mpyr][TFSI] electrolyte was also demonstrated in half cells [184]. Comparison with a similar cell operated in a 1 M $NaClO_4$ in an EC:DEC electrolyte shows that although the non-aqueous electrolyte performs much better at room temperature, the IL electrolyte displays very similar capacity and rate capability at temperatures as low as 50 °C. In addition to the improved thermal stability of the IL electrolyte (>400 °C), a much better cycle retention of 87% after 100 cycles was reported, compared to only 62% for the liquid electrolyte. Substitution of the TFSI anion by the FSI (bis(fluorosulfonyl) imide) anion allows a further decrease of the temperature. Half-cells assembled with $Na_{0.45}Ni_{0.22}Co_{0.11}Mn_{0.66}O_2$ as the positive electrode and either a NaTSFI-doped [C4mpyr]-[FSI] ionic liquid electrolyte or 0.5 M $NaPF_6$ in a PC-based non-aqueous electrolyte were compared. The reversible capacity at a rate of C/10 is slightly higher in the IL case [185], with a good retention of 80% of the capacity after 100 cycles, much higher than the non-aqueous cell. Other promising ionic liquids have yet to be tested for battery applications [186]. The published results show that when safety is a more important parameter than rate capability, ionic liquid electrolytes are a superior choice to traditional non-aqueous electrolytes, even for room-temperature applications.

7.1.4. Solid-state electrolytes

It has been recently shown that the solid state electrolytes such as gel polymer electrolytes and ceramic electrolytes can be considered as an excellent substitute for the liquid electrolytes, due to their most appealing feature of free standing consistency which contributes easy handling and cell design, modularity and reliability in various electrochemical devices.

Several kinds of electrolytes comprising a high dielectric constant plasticizer or solvent or its solution with different salts immobilized with the matrix of polymer hosts such as polyethylene oxide (PEO) [187,188], polyvinyl alcohol (PVA) [189], etc. have been reported.

Most of the reported gel polymer electrolytes comprise solvents such as propylene carbonate (PC), or ethylene carbonate (EC), but room temperature ionic liquids could also act as solvents to obtain thermally and electrochemically stable gel polymer electrolytes. A new sodium ion conducting gel polymer electrolyte based on the solution of sodium triflate ($NaCF_3SO_3$) in ionic liquid EMI-triflate immobilized with the host polymer PVdF-HFP has been recently reported by Kumar and Hashmi [190]. This gel polymer electrolyte showed high ionic conductivity at room temperature with a sufficiently wide electrochemical potential window and excellent thermal stability.

On the other hand, various research groups have reported composite/nanocomposite gel polymer electrolytes generated by the addition of the dispersion of micro- or nano-sized ceramic fillers. Bhide and Hariharan obtained a new Na^+ ion conducting polymer electrolyte $(PEO)_6$:$NaPO_3$ dispersed with 3–10 wt% $BaTiO_3$ fillers [191]. Aravindan et al. prepared sodium ion conducting composite polymer electrolytes by a solution casting technique in the skeleton of poly(vinylidene fluoride-co-hexafluoropropylene)/poly(ethyl methacrylate) (PVdF-HFP/PEMA) blend, with DC and EC as plasticizer and nanosized Sb_2O_3 as filler [192]. Finally, Kumar and Hashmi obtained gel polymer electrolyte nanocomposites based on poly(methylmethacrylate) (PMMA) and dispersed silica nanoparticles as fillers [128,192].

Ceramic solid materials would be another kind of electrolytes for Na batteries. The use of a solid electrolyte would eliminate the need for a separator, and avoid the use of organic electrolytes, leading to safer batteries and avoiding leakage risks. Moreover, ceramic materials could facilitate miniaturization and make battery design more versatile. Among the possible ceramic materials, sodium β-alumina solid electrolyte ceramic and NASICON phases stand out as possible electrolytes in Na batteries [193].

7.2. Mg-based batteries

Rechargeable Mg batteries have been long considered as a highly promising technology for energy storage and conversion, because Mg is the only element in the Periodic Table that could come close to lithium as an anode material of significance. Due to its bivalency, the specific volumetric capacity (3833 mAh cm^{-3}) is higher than that of lithium (2046 mAh cm^{-3}). Benefited by its low redox potential (−2.35 V *vs.* SHE or +0.65 V *vs.* Li), a gravimetric energy density (500 Wh kg^{-1}) close to or a volumetric energy density (1600 Wh L^{-1}) potentially higher than that of lithium is possible [194].

Development of anodically stable, ion conducting electrolyte solutions is a critical issue for the research of rechargeable Mg batteries. Aurbach and co-workers were the pioneers that conducted the trail-blazing research in this nascent battery chemistry [194–207]. They realized that the most severe challenge to a reversible Mg battery chemistry actually comes from the interfacial chemistry (or absence of it) on the metallic magnesium anode. Because of its divalent nature, Mg^{2+} cannot migrate through a SEI consisting of magnesium salts as does Li^+ through an SEI of corresponding lithium salts. The underlying reason for this difficulty is certainly not the size issue (0.74 Å of Mg^{2+} *vs.* 0.68 Å of Li^+) but the much stronger ionic attractions arising between Mg^{2+} and its counter-anions or coordination cages formed by solvent molecules. Thus, any feasible electrolyte for the Mg-battery must remain thermodynamically stable with metallic magnesium, ensuring that no reductions occur between Mg and any

electrolyte component. Moreover, any salt anions that might participate in the formation of interphases via electrochemical reduction should also be excluded, which cover perchlorates, triflates, hexafluorophosphate, etc. [77].

For primary or reserve Mg batteries, aqueous electrolytes such as sea water were commonly used because of the low redox potential and environmental friendliness of Mg. Mg primary batteries comprising chlorides, oxides, or O_2 as cathodes are commercially available, especially for marine use. For secondary batteries, Mg has to be reversibly deposited and stripped on Mg metal surfaces. No passivation films can be allowed on Mg anodes as the bivalent Mg ions cannot migrate through surface films comprising ionic magnesium compounds [207]. Most organic solvents (e.g. carbonates and nitriles) and normal salts (e.g. $Mg(ClO_4)_2$, $Mg(SO_3CF_3)_2$, and $Mg(N(SO_2CF_3)_2)_2$) are reduced to tenacious passivation films on Mg metal. The recent research advances on electrolytes for rechargeable Mg batteries includes 1) ethereal solutions, 2) ionic liquids, and 3) solid-state electrolytes.

7.2.1. Ethereal solutions

Reports of effective magnesium electrodeposition from Grignard reagents in ethereal solutions date back to the early part of the 20th century and have periodically appeared in the literature ever since [208–210]. Gregory et al. [211] first showed that solutions of organomagnesium compounds [magnesium tetrabutyl borate, $Mg(BBu_4)_2$] in tetrahydrofuran (THF) or primary amines (*N*-methylaniline) can be used as electrolytes in which both magnesium dissolution and deposition will occur at reasonable values of over-potentials. However, these electrolyte systems suffer from a narrow anodic stability window (<2 V), too narrow for practical utilization. Based on the concept that Gregory outlined in 1990, Aurbach et al. [194,205] in his pioneering work in 2000, proposed electrolytes based on magnesium organohaloaluminate salts, such as $Mg(AlCl_3R)_2$ and $Mg(AlCl_2RR')_2$, where R and R′ are alkyl groups in THF or polyethers of the glyme family. The most effective alkyl groups in this context are $-C_4H_9$ (butyl, Bu) and $-C_2H_5$ (ethyl, Et). The room temperature conductivity of these solutions at salt concentrations of approximately 0.3–0.5 M is high, in the range of several milli-siemens, comparable to the electrolytes used in Li batteries.

Zhu et al. [212] proposed a halogen-free boron based electrolyte ($Mg[Mes_3BPh]_2$/THF), which showed ionic conductivity 1.5×10^3 S cm^{-1}, highly reversible magnesium deposition/stripping on Ag metal electrode (1st cycle 80%, 15 cycle onwards 100%) and an oxidative stability up to 2.6 V on platinum and stainless steel electrodes. Carter et al. [213] synthesized a carborane based magnesium electrolyte [1-(1,7-carboranyl) magnesium chloride of formula $B_{10}C_2ClH_{11}Mg$] with a high oxidative stability by reacting m-carborane with isopropyl magnesium chloride (iPrMgCl). The carborane based electrolyte was found to be electrochemically stable up to 3.2 V on platinum (98% Coulombic efficiency for reversible Mg deposition/stripping), stainless steel (316 grade), and aluminum. Importantly, the electrolyte was tested with Mo_6S_8 model electrode and was able to deliver a capacity 45 mA h g^{-1} at a high rate of 100 mA g^{-1}. Besides, many ethereal solutions of Grignard reagents, $Mg(BR_2R'_2)_2$ (R, R′ = alkyl or aryl groups), $Mg(AX_{4-n}R_{n'}R'_{n''})_2$ complex (A = Al, B, Sb, P, As, Fe and Ta; X = Cl, Br and F; R, R′ = alkyl or aryl groups, $0 < n < 4$, $n' + n'' = n$) or amidomagnesium halides have been studied and summarized in pervious review papers [77,214,215]. Recently, non-organomagnesium salts such as $Mg(BH_4)_2$ and $MgB_{12}H_{12}$ have been considered highly competent electrolytes for magnesium-battery applications [213,216]. These electrolytes were compatible with Mg metal and provided excellent electrochemical performance in glyme.

7.2.2. Ionic liquids

ILs have wide electrochemical stability windows, low vapor pressures, and low flammabilities, making them attractive as replacements for organic solvents like THF and DME [217]. Furthermore, ILs enable the use of oxide-based cathodic materials, which show a superior specific capacity and operating voltage with respect to conventional Chevrel-phase materials. Nevertheless, results from prior studies of the electrochemistry of Mg salts in ILs have not been reproduced consistently. For example, Nuli et al. reported the electrodeposition of Mg from solutions of magnesium trifluoromethanesulfonate [$Mg(TfO)_2$, also called magnesium triflate] in imidazolium-based ILs [210,218–220], but other research groups have had difficulty replicating this finding [206,221]. Wang et al. reported both Mg plating and stripping from $Mg(TfO)_2$ dissolved in *N*-methyl-*N*-propylpiperidinium (PP_{13})–Tf_2N [220]. On the other hand, Cheek et al. reported that Mg could not be plated out of a mixture of $Mg(TfO)_2$ and 1-ethyl-3-methylimidazolium ($EMIM^+$) tetrafluoroborate (BF_4^-) [221]. Similarly, no Mg plating was observed when $Mg(Tf_2N)_2$ was dissolved in the quaternary ammonium IL *N*, *N*-diethyl-*N*-methyl(2-methoxyethyl)ammonium (DEME)–Tf_2N [222]. Furthermore, a report on $Mg(Tf_2N)_2$ in an *N*-butyl-*N*-methyl-pyrrolidinium-(Tf_2N) IL found that while intercalation reactions are possible with a magnesiated V_2O_5 cathode, it is unclear whether a Mg anode is compatible with this electrolyte [223]. Vardar et al. [224] investigated the electrochemistry of Borohydride (BH_4^-), trifluoromethanesulfonate (TfO^-), and bis(trifluoromethanesulfonyl)imide (Tf_2N^-) salts of Mg in three room temperature ionic liquid including l-*n*-butyl-3-methylimidazolium (BMIM)–Tf_2N, *N*-methyl-*N*-propylpiperidinium (PP_{13})–Tf_2N, and *N*,*N*-diethyl-*N*-methyl(2-methoxyethyl)-ammonium ($DEME^+$) tetrafluoroborate (BF_4^-) for application in Mg secondary Mg batteries. In solutions containing $BMIM^+$, oxidative activity near 0.8 V *vs.* Mg/Mg^{2+} is likely associated with the BMIM cation, rather than Mg stripping. The absence of voltammetric signatures of Mg plating from ILs with Tf_2N^- and BF_4^- suggests that strong Mg/anion Coulombic attraction inhibits electrodeposition. Co-solvent additions to $Mg(Tf_2N)_2/PP_{13}$–Tf_2N were explored but did not result in enhanced plating/stripping activity. The results highlight the need for IL solvents or co-solvent systems that promote Mg^{2+} dissociation. Recently, Bertasi et al. [225] synthesized high performance electrolytes

based on 1-ethyl-3-methylimidazolium chloride (EMImCl) doped with $AlCl_3$ and highly amorphous δ-$MgCl_2$. Mg anode cells assembled using the electrolytes were cyclically discharged at a high rate (35 mA g^{-1}), exhibiting an initial capacity of 80 mA h g^{-1} and a steady-state voltage of 2.3 V.

7.2.3. Solid-state electrolytes

Solid-state electrolytes for magnesium battery applications can be roughly classified into two categories: inorganic and polymer-based. Recently, it has been reported [226] that a $Mg(BH_4)(NH_2)$ solid state electrolyte can enable reversible Mg plating/stripping (but with a CE of less than 50% and conductivity of 10^{-6} Scm^{-1} at 150 °C). There is also a recent report using metal–organic frameworks as a solid Mg electrolyte, but no electrochemical data have been demonstrated [227].

Significant efforts have been devoted to polymer-based (such as poly(ethylene oxide), PEO) solid-state rechargeable Mg batteries [228–231]. However, most of the polymeric solid-state Mg electrolytes in the literature are based on simple Mg salts such as magnesium triflate $Mg(SO_3CF_3)_2$ [232] and magnesium(II) bis(trifluoromethanesulfonyl)imide $Mg(N(SO_2CF_3)_2)_2$ (or $Mg(TFSI)_2$) [233], similar to those for solid-state lithium electrolytes [234]. These salts are known to be incompatible with the Mg metal anode (*i.e.*, unable to produce reversible Mg plating/stripping) [207,235]; furthermore, it has been reported that the electrolytes based upon polymers and simple Mg salts are principally anion conductors (the transport number of Mg^{2+} being very low if not zero) because of the double charge and small size of Mg^{2+} [236]. There have been some efforts to increase the Mg^{2+} transference number, but no electrochemical properties, especially those pertaining to reversible Mg plating/stripping, have been reported [237,238]. There is one interesting report on solid-state Mg polymer electrolytes, consisting of PEO or PVDF and organometallic Mg complex salts, such as $Mg(AlEtBuCl_2)_2$/THF or tetraglyme, by Aurbach and coworkers [228] demonstrating reversible Mg plating/striping. Shao et al. [239] reported a nanocomposite polymer electrolyte based on poly(ethylene oxide) (PEO), $Mg(BH_4)_2$ and MgO nanoparticles for rechargeable Mg batteries. Cells with this electrolyte have a high coulombic efficiency of 98% for Mg plating/stripping and a high cycling stability.

7.3. Ca-based batteries

Calcium is a multivalent metal which is less reactive than lithium, has a high volumetric capacity of 2073 mAh L^{-1}, and is the fifth most abundant element in the earth's crust. In the 1980s, an extensive amount of research was devoted to the study of the electrochemistry of the Ca anode in inorganic polar aprotic solvents such as $SOCl_2$, SO_2, and SO_2Cl_2 [240–243].

While the electrochemistry of $Ca(AlCl_4)_2$ in $SOCl_2$ has been extensively studied there has been virtually less progress reported in the area of using calcium electrolytes in organic solvents with the goal of developing a rechargeable calcium battery. In 1991, Aurbach et al. investigated the behavior of calcium electrodes in electrolytes containing several organic solvents and salts [244]. They found that the surface chemical composition of the calcium anode was highly dependent on both the salt and the solvent used in the electrolyte. In solvents such as γ-butyrolactone (BL) and methyl formate (MF) the surface species include calcium butyrate derivatives of the γ-hydroxyl butyrate and cyclic β-ketone ester calcium salts. However, in acetonitrile, the calcium surface is covered by products formed from condensation of acetonitrile. In conclusion, calcium deposition (even at high negative potentials of −2.0 V *vs.* Ca) has not been observed in any electrolyte systems comprising $Ca(ClO_4)_2$ in organic solvents such as acetonitrile (AN), dimethylformamide (DMF), propylene carbonate (PC), BL, THF, and MF. This is presumably due to formation of a passivating layer formed by reduction of the salt and/or solvent which is apparently nonconductive with respect to calcium ions.

The current evolutionary level of a rechargeable calcium battery is rather primitive due to the primordial state of electrolyte development. The lack of useful calcium battery electrolytes limits the investigation of cathodes for a rechargeable calcium battery [214,245–247]. In the quest to develop a new calcium electrolyte one could envision exploring synthetic pathways which have been successful in obtaining electrolytes for another bivalent metal. Many of these synthetic approaches are based on Grignard reagents or organomagnesium compounds derived from Grignard reagents. This suggests that the corresponding calcium derivatives known as heavy Grignard reagents (RCaX, where R is alkyl or phenyl and X is iodide or bromide) would be an interesting starting point for investigating calcium electrolytes [214].

7.4. Zn-based batteries

For stationary purposes, energy storage systems with low material cost and reliable performance are required, where polyvalent ion charge carriers play a pivotal role. Rechargeable zinc batteries are considered as one of the best candidates for these applications, as they consist of environmentally friendly materials, such as manganese oxide cathodes, zinc metal anodes, and aqueous electrolyte systems containing $Zn(NO_3)_2$, $ZnSO_4$ or $ZnCl_2$ [248–254]. As for α-MnO_2, its discharge capacity is observed to be approximately 210 mA h g^{-1}, with a practical discharge potential of 1.3 V at a moderate current rate, leading to an energy density of 225 W h kg^{-1} based on the total weight of electrode materials. However, rechargeable zinc batteries employing tunneled manganese dioxide cathodes experience a sharp initial capacity fading and suffer poor performance at high current densities.

Most studies of Zn electrochemistry focus on the Zn-air batteries, which are cost-effective, with high energy density and promising energy storage devices for renewable energy and power sources for electric transportation. Selection of the proper electrolyte system is very important to achieving better performance.

Zinc–air batteries mostly operate in alkaline media, such as KOH and NaOH, for the sake of higher activity of both the zinc electrode and air electrode [254–259]. Potassium hydroxide is the most commonly used alkaline electrolyte because of its high conductivity, low viscosity, high activity for both the Zn and air electrodes, and good low temperature performance [258]. Most commonly, 7 M or 30 wt% KOH solution is employed for its maximum electric conductivity. In terms of Zn electrode failure, dendritic growth, shape change, passivation and self-discharge are the four main problems responsible for poor cycle life performance.

Recently, two main categories of non-aqueous electrolytes, *i.e.*, solid polymer electrolytes (SPEs) and room temperature ionic liquids (RTILs) have been investigated as alternative electrolyte systems. For zinc–air batteries, water loss from the liquid electrolytes is an important factor of performance degradation. It has been found that gelling of the electrolyte can help minimize the water loss, and enhance battery performance and life. SPEs are ionically conductive solids formed by dissolving conducting salt(s) into polymer(s) [260]. Othman et al. firstly investigated a SPE to immobilize KOH electrolyte for zinc–air batteries [261,262]. In a follow-up study, Mohamad demonstrated that a battery using 6 M KOH/hydroponics gel had an improved specific capacity of 657.5 mA h g^{-1} (789 W kg^{-1}) [263]. Recently, Fu and co-workers demonstrated a Zn–air battery fabricated by laminating a poly(vinyl alcohol) (PVA)-gelled electrolyte between an air electrode comprising a bifunctional catalyst loaded carbon cloth and a zinc film electrode, which exhibits excellent cycle stability over 120 cycles at the charge–discharge rate of 250 A L^{-1} (50 A kg^{-1}) without losing its functional performance even under extreme deformation. High volumetric energy density of 2905 W h L^{-1} and gravimetric energy density of 581 W h kg^{-1} were achieved, which demonstrates significant advantage over existing commercial bendable Zn–MnO_2 batteries and lithium-ion batteries [264].

For the Zn electrode side, aprotic room temperature ionic liquid (RTILs, without dissociable H^+ and unable to donate hydrogen), such as 1-butyl-1-methylpyrrolidinium bis(trifluoromethanesulfonyl)imide (BMPTFSI), 1-ethyl-3-methylimidazolium bis(trifluoromethanesulfonyl) imide (EMI-TFSI), 1-butyl-1-methylpyrrolidinium dicyanamide (BMP-DCA), 1-ethyl-3-methylimidazolium dicyanamide (EMIDCA) etc, have been proposed and evaluated [265–271]. Simons and co-workers investigated the electrodeposition and dissolution of Zn^{2+} in 1-ethyl-3-methylimidazolium dicyanamide ([EMIM][DCA]) ionic liquid [266]. The system had high current density and efficiency appropriate for use in rechargeable zinc batteries. Xu et al. studied the Zn/Zn(II) redox reactions in four aprotic RTILs based on pyrrolidinium ($[Pyrr]^+$) or imidazolium ($[Im]^+$) cations and bis(trifluoromethanesulfonyl)imide ($[TFSI]^-$) or dicyanamide ($[DCA]^-$) anions [267]. Cyclic voltammetry results suggest a smaller overpotential for Zn redox in $[Im]^+$ cation based and $[DCA]^-$ anion based RTILs than in $[Pyrr]^+$ and $[TFSI]^-$ based RTILs. Potentiodynamic polarization experiments indicate a strong dependence of the electrode reaction mechanism for the Zn species on the RTIL anions. In $[TFSI]^-$ based RTILs, Zn^{2+} ions are the electroactive species, with the electrode reaction being a single-step, two-electron transfer process. In $[DCA]^-$ based RTILs, two-step, single-electron reactions account for the electrode mechanism. The exchange current densities derived from Tafel analysis for the Zn species in the four RTILs are greater than 10^{-3} mA cm^{-2}, with the $[Im]^+$ cation based RTIL possessing the highest value of 9.9×10^{-3} mA cm^{-2}. However the performance of zinc air batteries using KOH as the electrolyte could not yet be approached by any aprotic electrolyte so far.

7.5. Al-based batteries

An aluminum (Al)-based battery, which involves three electron transfers during the electrochemical charge/discharge reactions, provides competitive storage capacity relative to the single-electron lithium-based battery [272]. Moreover, Al is the most abundant metal in the earth's crust and is more tolerant to water and air than Li. Because of its lower reactivity and easier handling, such an Al-based battery might offer significant cost savings and safety improvements over the lithium-battery platform. Thus, Al-based batteries have become one of the candidates for replacement the benchmark lithium batteries in portable electronic and large-scale grid for energy storage [121,273–278].

Choosing a right electrolyte is important for successful Al-battery technology. Up to date, aqueous solutions, non-aqueous organic electrolytes, ionic liquid and solid state electrolytes have been studied for Al batteries. Aqueous electrolytes are widely used in Al batteries because of their high ionic conductivities [276,278,279]. However, the standard reduction potential of Al^{3+} (1.68 V *vs.* standard hydrogen electrode) is lower than that of the hydrogen evolution reaction in an aqueous solution. Rechargeable research on aluminum batteries using aqueous solution electrolytes are unavoidable accompanied by hydrogen evolution reaction, which cannot be used in a closed system. Thus, electrolytes consisting of Al salts and organic solvents were investigated [121,280,281]. Reed et al. carried out CuHCF as a cathode material for aluminum ions in an electrolyte of aluminum trifluoromethanesulfonate (aluminum triflate) dissolved in diethylene glycol dimethyl ether (diglyme) [280]. The system shows initial discharge capacities as high as 60 mA h g^{-1} and reversible capacities between 5 and 14 mA h g^{-1}, with capacity typically fading after 10 to 15 cycles.

Rechargeable aluminum batteries working at room temperature was at a standstill until ionic liquids were used as electrolytes. Room Temperature Ionic Liquids (RTILs) with wide electrochemical window and high conductivity have been widely used in secondary batteries in recent years. $AlCl_3$ containing ionic liquids were used in rechargeable aluminum batteries as a priority, since no additional Al salts are necessary in these electrolytes. Rechargeable aluminum batteries that adopted $AlCl_3$ containing imidazolium ionic liquids ($AlCl_3$/[BMIM]Br, $AlCl_3$/[BMIM]Cl, $AlCl_3$/[BMIM]I, $AlCl_3$/[EMI]Cl, $AlCl_3$/[EMIM]Cl), etc. as electrolytes have been

studied and show stable electrochemical behavior [273,277,282–288]. Wang et al. found that anions may have a great effect on electrochemical properties of ionic liquids, as well as battery performance [282]. For a complete understanding of the anion-effect, haloaluminate containing ionic liquids prepared with different halogenated imidazole salt and $AlCl_3$/imidazolium chloride mole ratios are studied. When used as an electrolyte in a rechargeable aluminum battery with a V_2O_5 nanowire cathode, the $AlCl_3$/[BMIM]Cl ionic liquid with the mole ratio of 1.1: 1 shows the best performance. Cohn et al. investigated the Al–S battery comprised of a composite sulfur cathode, aluminum anode and an ionic liquid electrolyte of $AlCl_3$/1-ethyl-3-methylimidazolium chloride for the first time [277]. The Al/S battery exhibits a discharge voltage plateau of 1.1–1.2 V, with extremely high charge storage capacity of more than 1500 mAh g^{-1}, relative to the mass of sulfur in the cathode. The energy density of the Al/S cell is estimated to be 1700 Wh kg^{-1} sulfur, which is competitive with the most attractive battery chemistries targeted for high-energy electrochemical storage.

Similar with non-aqueous electrolytes, there are a few studies that have been carried out using solid state electrolytes in Al battery. The usage of solid state electrolyte is a new approach to prevent leakage challenge of this battery. Studies on Al-air batteries show that polymer host membranes that typically used in this battery are PAA, PVA or PEO-based gel doped with alkaline electrolyte [289]. The PAA/KOH with ZnO as corrosion inhibitor gives the highest ionic conductivity value (460 mS cm^{-1}) compared to other polymer host membranes. This battery peak capacity and energy density considering only Al can reach 1166 mAh g^{-1} and 1230 mWh g^{-1}, respectively, during constant current discharge. The battery prototype also exhibits a high power density of 91.13 mW cm^{-2}. Further studies focus on the conductivity, mechanical and thermal stabilities of the membrane need to be improved to increase the Al battery performance and durability.

8. Conclusion

In order to practically assess the viability of the rechargeable metal battery technology, optimization of each individual component including cathode, anode, separator and electrolyte is of course still urgently needed, and comprehensive studies enabling the building of laboratory-scale prototypes are compulsory. As an important component in rechargeable lithium and beyond lithium based batteries, five types of electrolytes on current investigation including non-aqueous organic electrolytes, aqueous solutions, ionic liquids, polymer and hybrid electrolytes have been introduced in this review. As the strongly reducing negative electrodes and strongly oxidizing positive electrodes require electrolyte solvents with large ESWs, which turns into the stringent and absolute demand that electrolyte solvents with active protons cannot be used. Besides, the electrolytes should also be stable, non-toxic, inexpensive, etc. Currently, most of the electrolytes used in rechargeable batteries are non-aqueous organic solutions. For aqueous electrolytes, the main disadvantage is the relatively low decomposition voltage, theoretically only 1.23 V. Ionic liquids (ILs) and polymer electrolytes have many properties of interest for safer and in some cases environmentally friendly batteries, such as non-volatility and non-flammability. However, their studies are still at a very early stage. In order to improve the properties of current electrolytes for practic use in rechargeable metal batteries, optimization methods such as varying the constituents of the electrolyte, metal salts, solvents, and additives, and their respective ratios should be furhter investigated.

Acknowledgements

Q. L. and J. C. contributed equally to this work. This work was supported by Chinese government under the “Thousand Youth Talents Program.”

References

[1] J.M. Tarascon, M. Armand, Nature 414 (2001) 359–367.
[2] J.B. Goodenough, Y. Kim, Chem. Mater. 22 (2010) 587–603.
[3] P.G. Bruce, B. Scrosati, J.M. Tarascon, Angew. Chem. Int. Ed. 47 (2008) 2930–2946.
[4] P.G. Bruce, S.A. Freunberger, L.J. Hardwick, J.-M. Tarascon, Nat. Mater. 11 (2012) 19–29.
[5] B.L. Ellis, K.T. Lee, L.F. Nazar, Chem. Mater. 22 (2010) 691–714.
[6] P. Roy, S.K. Srivastava, J. Mater. Chem. A 3 (2015) 2454–2484.
[7] K. Xu, Chem. Rev. 104 (2004) 4303–4418.
[8] J.R. Croy, A. Abouimrane, Z. Zhang, MRS Bull. 39 (2014) 407–415.
[9] Y. Li, B. Ravdel, B.L. Lucht, Electrochem. Solid State Lett. 13 (2010) A95–A97.
[10] L. Hu, Z. Zhang, K. Amine, J. Power Sources 236 (2013) 175–180.
[11] Z. Zhang, L. Hu, H. Wu, W. Weng, M. Koh, P.C. Redfern, L.A. Curtiss, K. Amine, Energy & Environ. Sci. 6 (2013) 1806–1810.
[12] P. Verma, P. Maire, P. Novák, Electrochim. Acta 55 (2010) 6332–6341.
[13] Z. Chen, Y. Ren, A.N. Jansen, C.K. Lin, W. Weng, K. Amine, Nat. Commun. 4 (2013) 66–78.
[14] A. von Cresce, K. Xu, J. Electrochem. Soc. 158 (2011) A337–A342.
[15] P. Yue, Z. Wang, X. Li, X. Xiong, J. Wang, X. Wu, H. Guo, Electrochim. Acta 95 (2013) 112–118.
[16] L. Li, Q. Yao, Z. Chen, L. Song, T. Xie, H. Zhu, J. Duan, K. Zhang, J. Alloys Compd. 650 (2015) 684–691.
[17] A. Manthiram, Y. Fu, Y.-S. Su, Acc. Chem. Res. 46 (2013) 1125–1134.
[18] B. Dunn, H. Kamath, J.M. Tarascon, Science 334 (2011) 928–935.
[19] R. Dominko, R. Demir-Cakan, M. Morcrette, J.-M. Tarascon, Electrochem. Commun. 13 (2011) 117–120.
[20] G. Jie, M.A. Lowe, Y. Kiya, H.D. Abruña, J. Phys. Chem. C 115 (2011) 25132–25137.
[21] Y.V. Mikhaylik, J.R. Akridge, J. Electrochem. Soc. 151 (2004) A1969–A1976.
[22] H. Yang, K. Kwon, T.M. Devine, J.W. Evans, J. Electrochem. Soc. 147 (2000) 4399–4407.
[23] L. Suo, Y.-S. Hu, H. Li, M. Armand, L. Chen, Nat. Commun. 4 (2013).
[24] X.-B. Cheng, J.-Q. Huang, H.-J. Peng, J.-Q. Nie, X.-Y. Liu, Q. Zhang, F. Wei, J. Power Sources 253 (2014) 263–268.
[25] J. Brückner, S. Thieme, H.T. Grossmann, S. Dörfler, H. Althues, S. Kaskel, J. Power Sources 268 (2014) 82–87.
[26] X. Liang, Z. Wen, Y. Liu, M. Wu, J. Jin, H. Zhang, X. Wu, J. Power Sources 196 (2011) 9839–9843.
[27] D. Aurbach, E. Pollak, R. Elazari, G. Salitra, C.S. Kelley, J. Affinito, J. Electrochem. Soc. 156 (2009) A694–A702.
[28] Z. Lin, Z. Liu, W. Fu, N.J. Dudney, C. Liang, Adv. Funct. Mater. 23 (2013) 1064–1069.

[29] W. Li, H. Yao, K. Yan, G. Zheng, Z. Liang, Y.-M. Chiang, Y. Cui, Nat. Commun. 6 (2015).
[30] C.-Z. Zhao, X.-B. Cheng, R. Zhang, H.-J. Peng, J.-Q. Huang, R. Ran, Z.-H. Huang, F. Wei, Q. Zhang, Energy Storage Mater. 3 (2016) 77–84.
[31] Y. Wang, J. Yi, Y. Xia, Adv. Energy Mater. 2 (2012) 830–840.
[32] N. Alias, A.A. Mohamad, J. Power Sources 274 (2015) 237–251.
[33] C. Wessells, R.A. Huggins, Y. Cui, J. Power Sources 196 (2011) 2884–2888.
[34] W. Li, J.R. Dahn, D.S. Wainwright, Science 264 (1994) 1115–1118.
[35] W. Li, W.R. McKinnon, J.R. Dahn, J. Electrochem. Soc. 141 (1994) 2310–2316.
[36] W. Li, J.R. Dahn, J. Electrochem. Soc. 142 (1995) 1742–1746.
[37] M. Zhao, B. Zhang, G. Huang, H. Zhang, X. Song, J. Power Sources 232 (2013) 181–186.
[38] J.-Y. Luo, W.-J. Cui, P. He, Y.-Y. Xia, Nat. Chem. 2 (2010) 760–765.
[39] X. Wang, Y. Hou, Y. Zhu, Y. Wu, R. Holze, Sci. Rep. 3 (2013).
[40] L. Suo, O. Borodin, T. Gao, M. Olguin, J. Ho, X. Fan, C. Luo, C. Wang, K. Xu, Science 350 (2015) 938–943.
[41] S.A. Freunberger, Y. Chen, Z. Peng, J.M. Griffin, L.J. Hardwick, F. Barde, P. Novak, P.G. Bruce, J. Am. Chem. Soc. 133 (2011) 8040–8047.
[42] S.A. Freunberger, Y. Chen, N.E. Drewett, L.J. Hardwick, F. Barde, P.G. Bruce, Angew. Chem. Int. Ed. 50 (2011) 8609–8613.
[43] N. Imanishi, O. Yamamoto, Mater. Today 17 (2014) 24–30.
[44] S. Visco, E. Nomon, B. Katz, L. Jongle, M. Chu, Nara, Japan, Abstract 53 (2004).
[45] Y. Shimonishi, T. Zhang, N. Imanishi, D. Im, D.J. Lee, A. Hirano, Y. Takeda, O. Yamamoto, N. Sammes, J. Power Sources 196 (2011) 5128–5132.
[46] M. Zhang, K. Takahashi, N. Imanishi, Y. Takeda, O. Yamamoto, B. Chi, J. Pu, J. Li, J. Electrochem. Soc. 159 (2012) A1114–A1119.
[47] H. Ohkuma, I. Uechi, M. Matsui, Y. Takeda, O. Yamamoto, N. Imanishi, J. Power Sources 245 (2014) 947–952.
[48] H. Zhou, Y. Wang, H. Li, P. He, ChemSusChem 3 (2010) 1009–1019.
[49] Frontmatter, in: Electrochemical Aspects of Ionic Liquids, John Wiley & Sons, Inc., 2005, pp. i–xiv.
[50] M. Armand, F. Endres, D.R. MacFarlane, H. Ohno, B. Scrosati, Nat. Mater. 8 (2009) 621–629.
[51] E. Zygadlo-Monikowska, Z. Florjanczyk, P. Kubisa, T. Biedron, W. Sadurski, A. Puczylowska, N. Langwald, J. Ostrowska, Int. J. Hydrogen Energy 39 (2014) 2943–2952.
[52] X.-G. Sun, C. Liao, N. Shao, J.R. Bell, B. Guo, H. Luo, D.-e. Jiang, S. Dai, J. Power Sources 237 (2013) 5–12.
[53] T. Mandai, H. Masu, M. Imanari, K. Nishikawa, J. Phys. Chem. B 116 (2012) 2059–2064.
[54] S. Ferrari, E. Quartarone, C. Tomasi, D. Ravelli, S. Protti, M. Fagnoni, P. Mustarelli, J. Power Sources 235 (2013) 142–147.
[55] Z. Wang, Y. Cai, Z. Wang, S. Chen, X. Lu, S. Zhang, J. Solid State Electrochem. 17 (2013) 2839–2848.
[56] H. Srour, L. Chancelier, E. Bolimowska, T. Gutel, S. Mailley, H. Rouault, C.C. Santini, J. Appl. Electrochem. 46 (2015) 149–155.
[57] M. Kärnä, M. Lahtinen, J. Valkonen, J. Mol. Struct. 922 (2009) 64–76.
[58] Y. Jin, S. Fang, L. Yang, S.-i. Hirano, K. Tachibana, J. Power Sources 196 (2011) 10658–10666.
[59] S. Seki, Y. Ohno, H. Miyashiro, Y. Kobayashi, A. Usami, Y. Mita, N. Terada, K. Hayamizu, S. Tsuzuki, M. Watanabe, J. Electrochem. Soc. 155 (2008) A421–A427.
[60] M.L.P. Le, L. Cointeaux, P. Strobel, J.-C. Leprêtre, P. Judeinstein, F. Alloin, J. Phys. Chem. C 116 (2012) 7712–7718.
[61] A. Lewandowski, A. Swiderska-Mocek, J. Appl. Electrochem. 40 (2009) 515–524.
[62] S. Fang, Z. Zhang, Y. Jin, L. Yang, S.-i. Hirano, K. Tachibana, S. Katayama, J. Power Sources 196 (2011) 5637–5644.
[63] G.B. Appetecchi, M. Montanino, D. Zane, M. Carewska, F. Alessandrini, S. Passerini, Electrochim. Acta 54 (2009) 1325–1332.
[64] N. Wongittharom, C.-H. Wang, Y.-C. Wang, G.T.-K. Fey, H.-Y. Li, T.-Y. Wu, T.-C. Lee, J.-K. Chang, J. Power Sources 260 (2014) 268–275.
[65] H. Li, J. Pang, Y. Yin, W. Zhuang, H. Wang, C. Zhai, S. Lu, RSC Adv. 3 (2013) 13907–13914.
[66] S. Fang, L. Yang, J. Wang, H. Zhang, K. Tachibana, K. Kamijima, J. Power Sources 191 (2009) 619–622.
[67] M. Chai, Y. Jin, S. Fang, L. Yang, S.-i. Hirano, K. Tachibana, J. Power Sources 216 (2012) 323–329.
[68] F. Wu, N. Chen, R. Chen, Q. Zhu, J. Qian, L. Li, Chem. Mater. 28 (2016) 848–856.
[69] L.X. Yuan, J.K. Feng, X.P. Ai, Y.L. Cao, S.L. Chen, H.X. Yang, Electrochem. Commun. 8 (2006) 610–614.
[70] L. Wang, H.R. Byon, J. Power Sources 236 (2013) 207–214.
[71] L. Wang, J. Liu, S. Yuan, Y. Wang, Y. Xia, Energy & Environ. Sci. 9 (2016) 224–231.
[72] T. Kuboki, T. Okuyama, T. Ohsaki, N. Takami, J. Power Sources 146 (2005) 766–769.
[73] F. Mizuno, S. Nakanishi, A. Shirasawa, K. Takechi, T. Shiga, H. Nishikoori, H. Iba, Electrochemistry 79 (2011) 876–881.
[74] G.A. Elia, J. Hassoun, W.J. Kwak, Y.K. Sun, B. Scrosati, F. Mueller, D. Bresser, S. Passerini, P. Oberhumer, N. Tsiouvaras, J. Reiter, Nano Lett. 14 (2014) 6572–6577.
[75] J.L. Schaefer, Y. Lu, S.S. Moganty, P. Agarwal, N. Jayaprakash, L.A. Archer, Appl. Nanosci. 2 (2011) 91–109.
[76] J.W. Fergus, J. Power Sources 195 (2010) 4554–4569.
[77] K. Xu, Chem. Rev. 114 (2014) 11503–11618.
[78] L.Y. Yang, D.X. Wei, M. Xu, Y.F. Yao, Q. Chen, Angew. Chem. 53 (2014) 3631–3635.
[79] Z. Zhu, M. Hong, D. Guo, J. Shi, Z. Tao, J. Chen, J. Am. Chem. Soc. 136 (2014) 16461–16464.
[80] W. Liu, N. Liu, J. Sun, P.C. Hsu, Y. Li, H.W. Lee, Y. Cui, Nano Lett. 15 (2015) 2740–2745.
[81] C. Tang, K. Hackenberg, Q. Fu, P.M. Ajayan, H. Ardebili, Nano Lett. 12 (2012) 1152–1156.
[82] R. Bouchet, S. Maria, R. Meziane, A. Aboulaich, L. Lienafa, J.-P. Bonnet, T.N.T. Phan, D. Bertin, D. Gigmes, D. Devaux, R. Denoyel, M. Armand, Nat. Mater. 12 (2013) 452–457.
[83] Y. Lu, M. Tikekar, R. Mohanty, K. Hendrickson, L. Ma, L.A. Archer, Adv. Energy Mater. 5 (2015) 1042073.
[84] P. Zhang, M. Li, B. Yang, Y. Fang, X. Jiang, G.M. Veith, X.G. Sun, S. Dai, Adv. Mater. 27 (2015) 8088–8094.
[85] L. Porcarelli, C. Gerbaldi, F. Bella, J.R. Nair, Sci. Rep. 6 (2016) 19892.
[86] C. Fasciani, S. Panero, J. Hassoun, B. Scrosati, J. Power Sources 294 (2015) 180–186.
[87] Y.Y.W.J.Y. Song, C.C. Wan, J. Power Sources 77 (1999) 183–197.
[88] J. Zhang, B. Sun, X. Huang, S. Chen, G. Wang, Sci. Rep. 4 (2014) 6007.
[89] P.-L. Kuo, C.-H. Tsao, C.-H. Hsu, S.-T. Chen, H.-M. Hsu, J. Membr. Sci. 499 (2016) 462–469.
[90] Y. Zhu, F. Wang, L. Liu, S. Xiao, Y. Yang, Y. Wu, Sci. Rep. 3 (2013) 3187.
[91] Y. Zhu, S. Xiao, Y. Shi, Y. Yang, Y. Hou, Y. Wu, Adv. Energy Mater. 4 (2014) 1300647.
[92] R. Prasanth, N. Shubha, H.H. Hng, M. Srinivasan, J. Power Sources 245 (2014) 283–291.
[93] N.H. Idris, M.M. Rahman, J.-Z. Wang, H.-K. Liu, J. Power Sources 201 (2012) 294–300.
[94] C.L. Yang, Z.H. Li, W.J. Li, H.Y. Liu, Q.Z. Xiao, G.T. Lei, Y.H. Ding, J. Membr. Sci. 495 (2015) 341–350.
[95] R. Prasanth, V. Aravindan, M. Srinivasan, J. Power Sources 202 (2012) 299–307.
[96] J. Yi, X. Liu, S. Guo, K. Zhu, H. Xue, H. Zhou, ACS Appl. Mater. Interfaces 7 (2015) 23798–23804.
[97] H. Bi, G. Sui, X. Yang, J. Power Sources 267 (2014) 309–315.
[98] Z. Zhang, G. Sui, H. Bi, X. Yang, J. Membr. Sci. 492 (2015) 77–87.
[99] W. Huang, Z. Zhu, L. Wang, S. Wang, H. Li, Z. Tao, J. Shi, L. Guan, J. Chen, Angew. Chem. 52 (2013) 9162–9166.
[100] S.S. Moganty, N. Jayaprakash, J.L. Nugent, J. Shen, L.A. Archer, Angew. Chem. 49 (2010) 9158–9161.
[101] J.K. Kim, J. Scheers, T.J. Park, Y. Kim, ChemSusChem 8 (2015) 636–641.

[102] S. Delacroix, F. Sauvage, M. Reynaud, M. Deschamps, S. Bruyère, M. Becuwe, D. Postel, J.-M. Tarascon, A.N. Van Nhien, Chem. Mater. 27 (2015) 7926–7933.
[103] Y. Lu, S.S. Moganty, J.L. Schaefer, L.A. Archer, J. Mater. Chem. 22 (2012) 4066.
[104] K.S. Korf, Y. Lu, Y. Kambe, L.A. Archer, J. Mater. Chem. A 2 (2014) 11866.
[105] Y. Lu, K. Korf, Y. Kambe, Z. Tu, L.A. Archer, Angew. Chem. 53 (2014) 488–492.
[106] Y. Lu, S.K. Das, S.S. Moganty, L.A. Archer, Adv. Mater. 24 (2012) 4430–4435.
[107] H.M. Kao, C.L. Chen, Angew. Chem. 43 (2004) 980–984.
[108] S.-K. Kim, D.-G. Kim, A. Lee, H.-S. Sohn, J.J. Wie, N.A. Nguyen, M.E. Mackay, J.-C. Lee, Macromolecules 45 (2012) 9347–9356.
[109] Q. Pan, D.M. Smith, H. Qi, S. Wang, C.Y. Li, Adv. Mater. 27 (2015) 5995–6001.
[110] A. Agrawal, S. Choudhury, L.A. Archer, RSC Adv. 5 (2015) 20800–20809.
[111] J.L. Nugent, S.S. Moganty, L.A. Archer, Adv. Mater. 22 (2010) 3677–3680.
[112] J.L. Schaefer, S.S. Moganty, D.A. Yanga, L.A. Archer, J. Mater. Chem. 21 (2011) 10094.
[113] S. Choudhury, R. Mangal, A. Agrawal, L.A. Archer, Nat. Commun. 6 (2015) 10101.
[114] N. Yabuuchi, K. Kubota, M. Dahbi, S. Komaba, Chem. Rev. 114 (2014) 11636–11682.
[115] H. Kim, J. Hong, K.Y. Park, H. Kim, S.W. Kim, K. Kang, Chem. Rev. 114 (2014) 11788–11827.
[116] V. Palomares, P. Serras, I. Villaluenga, K.B. Hueso, J. Carretero-Gonzalez, T. Rojo, Energy & Environ. Sci. 5 (2012) 5884–5901.
[117] M.D. Slater, D. Kim, E. Lee, C.S. Johnson, Adv. Funct. Mater. 23 (2013) 947–958.
[118] H. Pan, Y.-S. Hu, L. Chen, Energy & Environ. Sci. 6 (2013) 2338–2360.
[119] S.-W. Kim, D.-H. Seo, X. Ma, G. Ceder, K. Kang, Adv. Energy Mater. 2 (2012) 710–721.
[120] S. Komaba, W. Murata, T. Ishikawa, N. Yabuuchi, T. Ozeki, T. Nakayama, A. Ogata, K. Gotoh, K. Fujiwara, Adv. Funct. Mater. 21 (2011) 3859–3867.
[121] M. Mokhtar, M.Z.M. Talib, E.H. Majlan, S.M. Tasirin, W. Ramli, W.R.W. Daud, J. Sahari, J. Indus. Eng. Chem. 32 (2015) 1–20.
[122] T. Hashimoto, K. Hayashi, Electrochim. Acta 182 (2015) 809–814.
[123] P. Adelhelm, P. Hartmann, C.L. Bender, M. Busche, C. Eufinger, J. Janek, Beilstein J. Nanotechnol. 6 (2015) 1016–1055.
[124] S. Ha, J.-K. Kim, A. Choi, Y. Kim, K.T. Lee, ChemPhysChem 15 (2014) 1971–1982.
[125] S.K. Das, S. Lau, L.A. Archer, J. Mater. Chem. A 2 (2014) 12623–12629.
[126] X. Yu, A. Manthiram, ChemElectroChem 1 (2014) 1275–1280.
[127] A. Manthiram, X. Yu, Small 11 (2015) 2108–2114.
[128] D. Kumar, M. Suleman, S.A. Hashmi, Solid State Ionics 202 (2011) 45–53.
[129] G. Pang, C. Yuan, P. Nie, B. Ding, J. Zhu, X. Zhang, Nanoscale 6 (2014) 6328–6334.
[130] S. Il Park, I. Gocheva, S. Okada, J.-i. Yamaki, J. Electrochem. Soc. 158 (2011) A1067–A1070.
[131] J.F. Whitacre, A. Tevar, S. Sharma, Electrochem. Commun. 12 (2010) 463–466.
[132] A.D. Tevar, J.F. Whitacre, J. Electrochem. Soc. 157 (2010) A870–A875.
[133] Y.H. Jung, C.H. Lim, J.H. Kim, D.K. Kim, RSC Adv. 4 (2014) 9799–9802.
[134] X.Y. Wu, M.Y. Sun, Y.F. Shen, J.F. Qian, Y.L. Cao, X.P. Ai, H.X. Yang, ChemSusChem 7 (2014) 407–411.
[135] N. Arun, V. Aravindan, W.C. Ling, S. Madhavi, J. Alloys Compd. 603 (2014) 48–51.
[136] C.D. Wessells, M.T. Mcdowell, S.V. Peddada, M. Pasta, R.A. Huggins, C. Yi, ACS Nano 6 (2012) 1688–1694.
[137] F. Sauvage, E. Baudrin, J.M. Tarascon, Sensors Actuators B Chem. 120 (2007) 638–644.
[138] H. Qin, Z.P. Song, H. Zhan, Y.H. Zhou, J. Power Sources 249 (2014) 367–372.
[139] P. Moreau, D. Guyomard, J. Gaubicher, F. Boucher, Chem. Mater. 22 (2010) 4126–4128.
[140] M. Minakshi, D. Meyrick, J. Alloys Compd. 555 (2013) 10–15.
[141] M. Minakshi, D. Meyrick, D. Appadoo, Energy & Fuels 27 (2013) 3516–3522.
[142] F. Beck, P. Rüetschi, Electrochim. Acta 45 (2000) 2467–2482.
[143] A. Ponrouch, E. Marchante, M. Courty, J.-M. Tarascon, M. Rosa Palacin, Energy & Environ. Sci. 5 (2012) 8572–8583.
[144] R. Berthelot, D. Carlier, C. Delmas, Nat. Mater. 10 (2011), 74-U73.
[145] N. Yabuuchi, M. Kajiyama, J. Iwatate, H. Nishikawa, S. Hitomi, R. Okuyama, R. Usui, Y. Yamada, S. Komaba, Nat. Mater. 11 (2012) 512–517.
[146] I.D. Gocheva, M. Nishijima, T. Doi, S. Okada, J.I. Yamaki, T. Nishida, J. Power Sources 187 (2009) 247–252.
[147] N. Recham, J.N. Chotard, L. Dupont, K. Djellab, M. Armand, J.M. Tarascon, J. Electrochem. Soc. 156 (2009) A993–A999.
[148] X. Xia, J.R. Dahn, Electrochem. Solid-State Lett. 15 (2012).
[149] P. Thomas, J. Ghanbaja, D. Billaud, Electrochim. Acta 45 (1999) 423–430.
[150] P. Thomas, D. Billaud, Electrochim. Acta 47 (2002) 3303–3307.
[151] Y. Zhu, Y. Xu, Y. Liu, C. Luo, C. Wang, Nanoscale 5 (2012) 780–787.
[152] A. Bhide, J. Hofmann, A. Katharina Durr, J. Janek, P. Adelhelm, Phys. Chem. Chem. Phys. 16 (2014) 1987–1998.
[153] R. Alcántara, J.M.J. Mateos, J.L. Tirado, J. Electrochem. Soc. 149 (2002) A201–A205.
[154] Y. Cao, L. Xiao, W. Wang, D. Choi, Z. Nie, J. Yu, L.V. Saraf, Z. Yang, J. Liu, Adv. Mater. 23 (2011) 3155–3160.
[155] R. Alcántara, J.M. Jiménez-Mateos, P. Lavela, J.L. Tirado, Electrochem. Commun. 3 (2001) 639–642.
[156] J. Barker, M.Y. Saidi, J.L. Swoyer, Electrochem. solid-state Lett. 6 (2003).
[157] R. Alcántara, P. Lavela, G.F. Ortiz, J.L. Tirado, Electrochem. Solid State Lett. 8 (2005) A222–A225.
[158] H. Zhuo, X. Wang, A. Tang, Z. Liu, S. Gamboa, P.J. Sebastian, J. Power Sources 160 (2006) 698–703.
[159] D.A. Stevens, J.R. Dahn, J. Electrochem. Soc. 147 (2000) 1271–1273.
[160] H. Liu, H. Zhou, L. Chen, Z. Tang, W. Yang, J. Power Sources 196 (2011) 814–819.
[161] C. Vidal-Abarca, P. Lavela, J.L. Tirado, A.V. Chadwick, M. Alfredsson, E. Kelder, J. Power Sources 197 (2012) 314–318.
[162] L.W. Shacklette, T.R. Jow, L. Townsend, J. Electrochem. Soc. 135 (1988) 2669–2674.
[163] S. Wenzel, T. Hara, J. Janek, P. Adelhelm, Energy & Environ. Sci. 4 (2011) 3342–3345.
[164] D.A. Stevens, J.R. Dahn, J. Electrochem. Soc. 147 (2000) 4428–4431.
[165] L.D. Ellis, T.D. Hatchard, M.N. Obrovac, J. Electrochem. Soc. 159 (2012) A1801–A1805.
[166] H. Ryu, T. Kim, K. Kim, J.H. Ahn, T. Nam, G. Wang, H.J. Ahn, J. Power Sources 196 (2011) 5186–5190.
[167] P. Hartmann, C.L. Bender, J. Sann, A.K. Dürr, M. Jansen, J. Janek, P. Adelhelm, Phys. Chem. Chem. Phys. 15 (2013) 11661–11672.
[168] M. Vračar, A.K. Dürr, A. Garsuch, J. Janek, P. Adelhelm, Nat. Mater. 12 (2013) 228–232.
[169] S. Wenzel, H. Metelmann, C. Raiß, A.K. Dürr, J. Janek, P. Adelhelm, J. Power Sources 243 (2013) 758–765.
[170] X. Xia, W.M. Lamanna, J.R. Dahn, J. Electrochem. Soc. 160 (2013) A607–A609.
[171] A. Plewa-Marczewska, T. Trzeciak, A. Bitner, L. Niedzicki, M. Dranka, G.Z. Żukowska, M. Marcinek, W. Wieczorek, Chem. Mater. 26 (2014) 4908–4914.
[172] G. Singh, F. Aguesse, L. Otaegui, E. Goikolea, E. Gonzalo, J. Segalini, T. Rojo, J. Power Sources 273 (2015) 333–339.
[173] L. Otaegui, E. Goikolea, F. Aguesse, M. Armand, T. Rojo, G. Singh, J. Power Sources 297 (2015) 168–173.

[174] H. Pan, X. Lu, X. Yu, Y.-S. Hu, H. Li, X.-Q. Yang, L. Chen, Adv. Energy Mater. 3 (2013) 1186–1194.
[175] C. Ge, L. Wang, L. Xue, Z.-S. Wu, H. Li, Z. Gong, X.-D. Zhang, J. Power Sources 248 (2014) 77–82.
[176] J. Chen, Z. Huang, C. Wang, S. Porter, B. Wang, W. Lie, H.K. Liu, Chem. Commun. 51 (2015) 9809–9812.
[177] L.J. Krause, W. Lamanna, J. Summerfield, M. Engle, G. Korba, R. Loch, R. Atanasoski, J. Power Sources 68 (1997) 320–325.
[178] A. Ponrouch, R. Dedryvere, D. Monti, A.E. Demet, J.M.A. Mba, L. Croguennec, C. Masquelier, P. Johansson, M.R. Palacin, Energy & Environ. Sci. 6 (2013) 2361–2369.
[179] A. Fukunaga, T. Nohira, R. Hagiwara, K. Numata, E. Itani, S. Sakai, K. Nitta, S. Inazawa, J. Power Sources 246 (2014) 387–391.
[180] C. Ding, T. Nohira, R. Hagiwara, A. Fukunaga, S. Sakai, K. Nitta, Electrochim. Acta 176 (2015) 344–349.
[181] S.A.M. Noor, P.C. Howlett, D.R. Macfarlane, M. Forsyth, Electrochim. Acta 114 (2013) 766–771.
[182] H. Yoon, H. Zhu, A. Hervault, M. Armand, D.R. Macfarlane, M. Forsyth, Phys. Chem. Chem. Phys. 16 (2014) 12350–12355.
[183] C. Ding, T. Nohira, K. Kuroda, R. Hagiwara, A. Fukunaga, S. Sakai, K. Nitta, S. Inazawa, J. Power Sources 238 (2013) 296–300.
[184] N. Wongittharom, T.C. Lee, C.H. Wang, Y.C. Wang, J.K. Chang, J. Mater. Chem. A 2 (2014) 5655–5661.
[185] L.G. Chagas, D. Buchholz, L. Wu, B. Vortmann, S. Passerini, J. Power Sources 247 (2014) 377–383.
[186] D. Monti, E. Jónsson, M.R. Palacín, P. Johansson, J. Power Sources 245 (2014) 630–636.
[187] S.R. Mohapatra, A.K. Thakur, R.N.P. Choudhary, Ionics 14 (2008) 255–262.
[188] V.M. Mohan, V. Raja, P.B. Bhargav, A.K. Sharma, V.V.R.N. Rao, J. Polym. Res. 14 (2007) 283–290.
[189] P.B. Bhargav, V.M. Mohan, A.K. Sharma, V.V.R.N. Rao, Ionics 13 (2007) 441–446.
[190] D. Kumar, S.A. Hashmi, Solid State Ionics 181 (2010) 416–423.
[191] A. Bhide, K. Hariharan, Polym. Int. 57 (2008) 523–529.
[192] V. Aravindan, C. Lakshmi, P. Vickraman, Curr. Appl. Phys. 9 (2009) 1106–1111.
[193] J.F.M. Oudenhoven, L. Baggetto, P.H.L. Notten, Adv. Energy Mater. 1 (2011) 10–33.
[194] D. Aurbach, Z. Lu, A. Schechter, Y. Gofer, H. Gizbar, R. Turgeman, Y. Cohen, M. Moshkovich, E. Levi, Nature 407 (2000) 724–727.
[195] D. Aurbach, S.G. S., E. Levi, A. Mitelman, O. Mizrahi, O. Chusid, M. Brunelli, Adv. Mater. 19 (2007) 4260–4267.
[196] H.D. Yoo, I. Shterenberg, Y. Gofer, G. Gershinsky, N. Pour, D. Aurbach, Energy & Environ. Sci. 6 (2013) 2265–2279.
[197] Y. Vestfried, O. Chusid, Y. Goffer, P. Aped, D. Aurbach, Organometallics 26 (2007) 3130–3137.
[198] I. Shterenberg, M. Salama, H.D. Yoo, Y. Gofer, J.-B. Park, Y.-K. Sun, D. Aurbach, J. Electrochem. Soc. 162 (2015) A7118–A7128.
[199] N. Pour, Y. Gofer, D.T. Major, K. Keinan-Adamsky, H.E. Gottlieb, D. Aurbach, Organometallics 32 (2013) 3165–3173.
[200] N. Pour, Y. Gofer, D.T. Major, D. Aurbach, J. Am. Chem. Soc. 133 (2011) 6270–6278.
[201] O. Mizrahi, N. Amir, E. Pollak, O. Chusid, V. Marks, H. Gottlieb, L. Larush, E. Zinigrad, D. Aurbach, J. Electrochem. Soc. 155 (2008) A103–A109.
[202] Y. Gofer, O. Chusid, H. Gizbar, Y. Viestfrid, H.E. Gottlieb, V. Marks, D. Aurbach, Electrochem. Solid State Lett. 9 (2006) A257–A260.
[203] R.E. Doe, R. Han, J. Hwang, A.J. Gmitter, I. Shterenberg, H.D. Yoo, N. Pour, D. Aurbach, Chem. Commun. 50 (2014) 243–245.
[204] D. Aurbach, I. Weissman, Y. Gofer, E. Levi, Chem. Rec. 3 (2003) 61–73.
[205] D. Aurbach, H. Gizbar, A. Schechter, O. Chusid, H.E. Gottlieb, Y. Gofer, I. Goldberg, J. Electrochem. Soc. 149 (2002) A115–A121.
[206] N. Amir, Y. Vestfrid, O. Chusid, Y. Gofer, D. Aurbach, J. Power Sources 174 (2007) 1234–1240.
[207] Z. Lu, A. Schechter, M. Moshkovich, D. Aurbach, J. Electroanal. Chem. 466 (1999) 203–217.
[208] L.W. Gaddum, H.E. French, J. Am. Chem. Soc. 49 (1927) 1295–1299.
[209] J.H. Conner, W.E. Reid, G.B. Wood, J. Electrochem. Soc. Absorbed Electrochem. Technol. 104 (1957).
[210] Z. Feng, Y. Nuli, J. Wang, J. Yang, J. Electrochem. Soc. 153 (2006) C689–C693.
[211] T.D. Gregory, R.J. Hoffman, R.C. Winterton, J. Electrochem. Soc. 137 (3) (1990) 775–780.
[212] J. Zhu, Y. Guo, J. Yang, Y. Nuli, F. Zhang, J. Wang, S.-i. Hirano, J. Power Sources 248 (2014) 690–694.
[213] T.J. Carter, R. Mohtadi, T.S. Arthur, F. Mizuno, R. Zhang, S. Shirai, J.W. Kampf, Angew. Chem. Int. Ed. 53 (2014) 3173–3177.
[214] J. Muldoon, C.B. Bucur, T. Gregory, Chem. Rev. 114 (2014) 11683–11720.
[215] P. Saha, M.K. Datta, O.I. Velikokhatnyi, A. Manivannan, D. Alman, P.N. Kumta, Prog. Mater. Sci. 66 (2014) 1–86.
[216] R. Mohtadi, M. Matsui, T.S. Arthur, S.-J. Hwang, Angew. Chem. Int. Ed. 51 (2012) 9780–9783.
[217] D.R. Macfarlane, N. Tachikawa, M. Forsyth, J.M. Pringle, P.C. Howlett, G.D. Elliott, J.H. Davis, M. Watanabe, P. Simon, C.A. Angell, Energy & Environ. Sci. 7 (2014) 232–250.
[218] Y. Nuli, J. Yang, R. Wu, Electrochem. Commun. 7 (2005) 1105–1110.
[219] Y. Nuli, J. Yang, P. Wang, Appl. Surf. Sci. 252 (2006) 8086–8090.
[220] P. Wang, Y. Nuli, J. Yang, Z. Feng, Surf. Coat. Technol. 201 (2006) 3783–3787.
[221] G.T. Cheek, W.E. O'Grady, S.Z.E. Abedin, E.M. Moustafa, F. Endres, J. Electrochem. Soc. 155 (2008) D91–D95.
[222] O. Shimamura, N. Yoshimoto, M. Matsumoto, M. Egashia, M. Morita, J. Power Sources 196 (2011) 1586–1588.
[223] G.A. Giffin, A. Moretti, S. Jeong, S. Passerini, J. Phys. Chem. C 118 (2014) 9966–9973.
[224] G. Vardar, A.E.S. Sleightholme, J. Naruse, H. Hiramatsu, D.J. Siegel, C.W. Monroe, ACS Appl. Mater. Interfaces 6 (2014) 18033–18039.
[225] F. Bertasi, C. Hettige, F. Sepehr, X. Bogle, G. Pagot, K. Vezzu, E. Negro, S.J. Paddison, S.G. Greenbaum, M. Vittadello, V. Di Noto, ChemSusChem 8 (2015) 3069–3076.
[226] S. Higashi, K. Miwa, M. Aoki, K. Takechi, Chem. Commun. 50 (2014) 1320–1322.
[227] M.L. Aubrey, R. Ameloot, B.M. Wiers, J.R. Long, Energy & Environ. Sci. 7 (2014) 667–671.
[228] O. Chusid, Y. Gofer, H. Gizbar, Y. Vestfrid, E. Levi, D. Aurbach, I. Riech, Adv. Mater. 15 (2003) 627–630.
[229] G.G. Kumar, N. Munichandraiah, Electrochim. Acta 47 (2002) 1013–1022.
[230] M. Sundar, S. Selladurai, Ionics 12 (2006) 281–286.
[231] A.R. Polu, R. Kumar, K.V. Kumar, N.K. Jyothi, in: Solid State Physics: Proceedings of the 57th DAE Solid State Physics Symposium 2012, 2013, pp. 996–997.
[232] V. Aravindan, G. Karthikaselvi, P. Vickraman, S.P. Naganandhini, J. Appl. Polym. Sci. 112 (2009) 3024–3029.
[233] N. Yoshimoto, S. Yakushiji, M. Ishikawa, M. Morita, Electrochim. Acta 48 (2003) 2317–2322.
[234] E. Quartarone, P. Mustarelli, Chem. Soc. Rev. 40 (2011) 2525–2540.
[235] I. Shterenberg, M. Salama, Y. Gofer, E. Levi, D. Aurbach, MRS Bull. 39 (2014) 453–460.
[236] C. Liebenow, A. Reiche, P. Lobitz, Electrochim. Acta 40 (1995) 2375–2378.
[237] M. Saito, H. Ikuta, Y. Uchimoto, M. Wakihara, S. Yokoyama, T. Yabe, M. Yamamoto, J. Electrochem. Soc. 150 (2003) A477–A483.
[238] M. Saito, H. Ikuta, Y. Uchimoto, M. Wakihara, S. Yokoyama, T. Yabe, M. Yamamoto, J. Phys. Chem. B 107 (2003) 11608–11614.
[239] Y. Shao, N.N. Rajput, J. Hu, M. Hu, T. Liu, Z. Wei, M. Gu, X. Deng, S. Xu, K.S. Han, J. Wang, Z. Nie, G. Li, K.R. Zavadil, J. Xiao, C. Wang, W.A. Henderson, J.-G. Zhang, Y. Wang, K.T. Mueller, K. Persson, J. Liu, Nano Energy 12 (2015) 750–759.
[240] A. Meitav, E. Peled, J. Electrochem. Soc. 129 (1982) 451–457.
[241] E. Peled, A. Meitav, M. Brand, J. Electrochem. Soc. 128 (1981) 1936–1938.
[242] R.J. Staniewicz, J. Electrochem. Soc. 127 (1979) 782–789.

[243] C.W. Walker, W.L. Wade, M. Binder, J. Power Sources 25 (1989) 187–193.
[244] D. Aurbach, R. Skaletsky, Y. Gofer, J. Electrochem. Soc. 138 (1991) 3536–3545.
[245] H. Yin, D. Tang, X. Mao, W. Xiao, D. Wang, J. Mater. Chem. A 3 (2015) 15184–15189.
[246] P. Padigi, G. Goncher, D. Evans, R. Solanki, J. Power Sources 273 (2015) 460–464.
[247] K.A. See, J.A. Gerbec, Y.-S. Jun, F. Wudl, G.D. Stucky, R. Seshadri, Adv. Energy Mater. 3 (2013) 1056–1061.
[248] L. Zhang, L. Chen, X. Zhou, Z. Liu, Sci. Rep. 5 (2015).
[249] R. Trocoli, F. La Mantia, ChemSusChem 8 (2015) 481–485.
[250] M.H. Alfaruqi, V. Mathew, J. Gim, S. Kim, J. Song, J.P. Baboo, S.H. Choi, J. Kim, Chem. Mater. 27 (2015) 3609–3620.
[251] C. Xu, B. Li, H. Du, F. Kang, Angew. Chem. Int. Ed. 51 (2012) 933–935.
[252] B. Lee, H.R. Lee, H. Kim, K.Y. Chung, B.W. Cho, S.H. Oh, Chem. Commun. 51 (2015) 9265–9268.
[253] Z. Jia, B. Wang, Y. Wang, Mater. Chem. Phys. 149 (2015) 601–606.
[254] K. Wang, P. Pei, Z. Ma, H. Chen, H. Xu, D. Chen, X. Wang, J. Mater. Chem. A 3 (2015) 22648–22655.
[255] Y. Li, M. Gong, Y. Liang, J. Feng, J.-E. Kim, H. Wang, G. Hong, B. Zhang, H. Dai, Nat. Commun. 4 (2013).
[256] G. Du, X. Liu, Y. Zong, T.S.A. Hor, A. Yu, Z. Liu, Nanoscale 5 (2013) 4657–4661.
[257] D.U. Lee, J.-Y. Choi, K. Feng, H.W. Park, Z. Chen, Adv. Energy Mater. 4 (2014).
[258] Yanguang Li, Hongjie Dai, Chem. Soc. Rev. 43 (2014) 5257–5275.
[259] X. Liu, M. Park, M.G. Kim, S. Gupta, G. Wu, J. Cho, Angew. Chem. Int. Ed. 54 (2015) 9654–9658.
[260] N. Vassal, E. Salmon, J.F. Fauvarque, Electrochim. Acta 45 (2000) 1527–1532.
[261] R. Othman, W.J. Basirun, A.H. Yahaya, A.K. Arof, J. Power Sources 103 (2001) 34–41.
[262] R. Othman, A.H. Yahaya, A.K. Arof, J. New Mater. Electrochem. Syst. 5 (2002) 177–182.
[263] A.A. Mohamad, J. Power Sources 159 (2006) 752–757.
[264] J. Fu, U.L. Dong, F.M. Hassan, L. Yang, Z. Bai, M.G. Park, Z. Chen, Adv. Mater. (2015) 5617–5622.
[265] M. Xu, D.G. Ivey, Z. Xie, W. Qu, J. Power Sources 283 (2015) 358–371.
[266] T.J. Simons, A.A.J. Torriero, P.C. Howlett, D.R. Macfarlane, M. Forsyth, Electrochem. Commun. 18 (2012) 119–122.
[267] M. Xu, D.G. Ivey, Z. Xie, W. Qu, Electrochim. Acta 89 (2013) 756–762.
[268] C.O. Laoire, S. Mukerjee, K.M. Abraham, E.J. Plichta, M.A. Hendrickson, J. Phys. Chem. C 114 (2010) 9178–9186.
[269] G. Girishkumar, B. Mccloskey, A.C. Luntz, S. Swanson, W. Wilcke, J. Phys. Chem. Lett. 1 (2010) 2193–2203.
[270] M. Kar, T.J. Simons, M. Forsyth, D.R. MacFarlane, Phys. Chem. Chem. Phys. 16 (2014) 18658–18674.
[271] M. Kar, B. Winther-Jensen, M. Forsyth, D.R. MacFarlane, Phys. Chem. Chem. Phys. 15 (2013) 7191–7197.
[272] Q. Li, N.J. Bjerrum, Q. Li, N.J. Bjerrum, J. Power Sources 110 (2002) 1–10.
[273] N. Jayaprakash, S.K. Das, L.A. Archer, Chem. Commun. 47 (2011) 12610–12612.
[274] D.R. Egan, C.P.D. León, R.J.K. Wood, R.L. Jones, K.R. Stokes, F.C. Walsh, J. Power Sources 236 (2013) 293–310.
[275] M.C. Lin, M. Gong, B.G. Lu, Y.P. Wu, D.Y. Wang, M.Y. Guan, M. Angell, C.X. Chen, J. Yang, B.J. Hwang, H.J. Dai, Nature 520 (2015) 325-+.
[276] Y.J. He, J.F. Peng, W. Chu, Y.Z. Li, D.G. Tong, J. Mater. Chem. A 2 (2014) 1721–1731.
[277] G. Cohn, L. Ma, L.A. Archer, J. Power Sources 283 (2015) 416–422.
[278] S. Liu, J.J. Hu, N.F. Yan, G.L. Pan, G.R. Li, X.P. Gao, Energy & Environ. Sci. 5 (2012) 9743–9746.
[279] S. Liu, G.L. Pan, G.R. Li, X.P. Gao, J. Mater. Chem. A 3 (2014) 959–962.
[280] L.D. Reed, Chem. Commun. 51 (2015).
[281] T. Mandai, P. Johansson, J. Mater. Chem. A 3 (2015) 12230–12239.
[282] H.L. Wang, S.C. Gu, Y. Bai, S. Chen, N. Zhu, C. Wu, F. Wu, J. Mater. Chem. A 3 (2015) 22677–22686.
[283] H.B. Sun, W. Wang, Z.J. Yu, Y. Yuan, S. Wang, S.Q. Jiao, Chem. Commun. 51 (2015) 11892–11895.
[284] M. Chiku, H. Takeda, S. Matsumura, E. Higuchi, H. Inoue, ACS Appl. Mater. Interfaces 7 (2015) 24385–24389.
[285] G. Kamath, B. Narayanan, S. Sankaranarayanan, Phys. Chem. Chem. Phys. 16 (2014) 20387–20391.
[286] W. Wang, B. Jiang, W. Xiong, H. Sun, Z. Lin, L. Hu, J. Tu, J. Hou, H. Zhu, S. Jiao, Sci. Rep. 3 (2013) 1119–1120.
[287] L.D. Reed, E. Menke, J. Electrochem. Soc. 160 (2013) A915–A917.
[288] J.V. Rani, V. Kanakaiah, T. Dadmal, M.S. Rao, S. Bhavanarushi, J. Electrochem. Soc. 160 (2013) A1781–A1784.
[289] Z. Zhang, C.C. Zuo, Z.H. Liu, Y. Yu, Y.X. Zuo, Y. Song, J. Power Sources 251 (2014) 470–475.